Article

Immunity

Induction of IL-10-producing type 2 innate lymphoid cells by allergen immunotherapy is associated with clinical response

Graphical Abstract

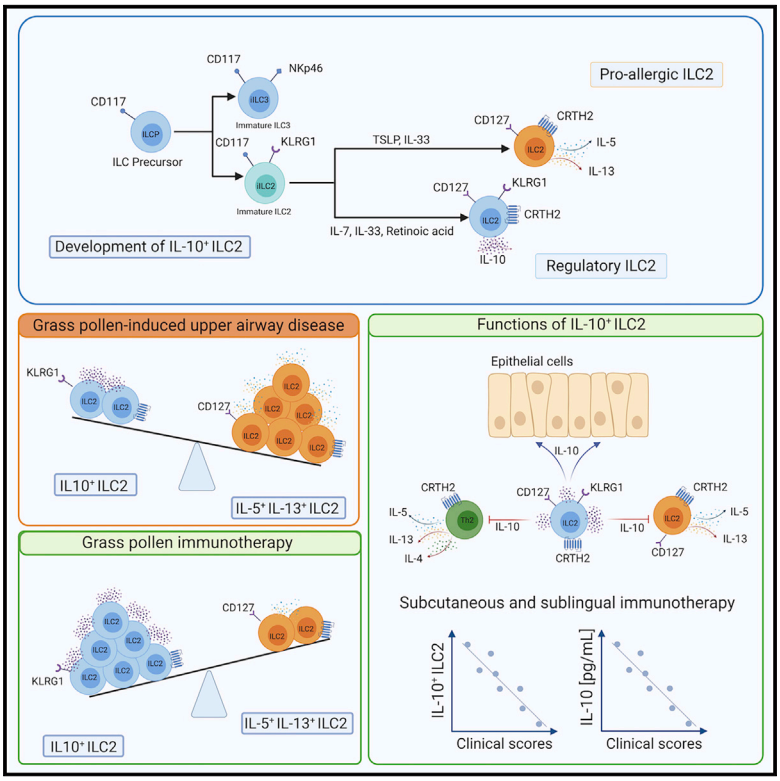

Highlights

- A thorough characterization of IL-10-producing type 2 innate lymphoid cell (ILC2s)
- IL-10-producing ILC2s restore epithelial cell integrity and suppress Th2 responses
- Symptom severity inversely correlates with IL-10-producing ILC2s after immunotherapy
- IL-10-producing ILC2s play a critical role in tolerance induction to aeroallergens

Authors

Korneliusz Golebski, Janice A. Layhadi, Umit Sahiner, ..., Stephen R. Durham, Hergen Spits, Mohamed H. Shamji

Correspondence

hergen.spits@amsterdamumc.nl (H.S.), m.shamji@imperial.ac.uk (M.H.S.)

In Brief

Underpinning mechanisms of immune tolerance following allergen immunotherapy is not well understood. Golebski et al. characterized IL-10-producing type 2 innate lymphoid cell and report that these cells with regulatory properties are induced following immunotherapy suggesting that they play an essential role in immune tolerance to aeroallergens in upper respiratory disease.

Golebski et al., 2021, Immunity *54*, 291–307
February 9, 2021
https://doi.org/10.1016/j.immuni.2020.12.013

CellPress

Immunity

CellPress

Article

Induction of IL-10-producing type 2 innate lymphoid cells by allergen immunotherapy is associated with clinical response

Korneliusz Golebski,[1,2,11] Janice A. Layhadi,[3,4,11] Umit Sahiner,[3] Esther H. Steveling-Klein,[3,5] Madison M. Lenormand,[3,4] Rachael C.Y. Li,[3,4] Suzanne M. Bal,[1] Balthasar A. Heesters,[1] Gemma Vilà-Nadal,[3] Oliver Hunewald,[6] Guillem Montamat,[6,7] Feng Q. He,[6,8] Markus Ollert,[6,9] Oleksandra Fedina,[3] Mongkol Lao-Araya,[3] Susanne J.H. Vijverberg,[2] Anke-Hilse Maitland-van der Zee,[2] Cornelis M. van Drunen,[10] Wytske J. Fokkens,[10] Stephen R. Durham,[3,4] Hergen Spits,[1,*] and Mohamed H. Shamji[3,4,12,*]

[1]Department of Experimental Immunology, Amsterdam UMC, University of Amsterdam, Amsterdam, the Netherlands
[2]Department of Respiratory Medicine, Amsterdam UMC, University of Amsterdam, Amsterdam, the Netherlands
[3]Immunomodulation and Tolerance Group, Allergy and Clinical Immunology, Department of National Heart and Lung Institute, Imperial College London, London, UK
[4]NIHR Biomedical Research Centre, Asthma UK Centre in Allergic Mechanisms of Asthma, London, Imperial College London, London, UK
[5]Department of Dermatology, Allergy Unit, University Hospital Basel, Basel, Switzerland
[6]Department of Infection and Immunity, Luxembourg Institute of Health (LIH), 29, rue Henri Koch, 4354 Esch-sur-Alzette, Luxembourg
[7]Department of Clinical Research, Faculty of Health Sciences, University of Southern Denmark, Odense, Denmark
[8]Institute of Medical Microbiology, University Hospital Essen, University Duisburg-Essen, 45122 Essen, Germany
[9]Department of Dermatology and Allergy Center, Odense Research Centre for Anaphylaxis (ORCA), University of Southern Denmark, Odense, Denmark
[10]Department of Otorhinolaryngology, Amsterdam UMC, University of Amsterdam, Amsterdam, the Netherlands
[11]These authors contributed equally
[12]Lead contact
*Correspondence: hergen.spits@amsterdamumc.nl (H.S.), m.shamji@imperial.ac.uk (M.H.S.)
https://doi.org/10.1016/j.immuni.2020.12.013

SUMMARY

The role of innate immune cells in allergen immunotherapy that confers immune tolerance to the sensitizing allergen is unclear. Here, we report a role of interleukin-10-producing type 2 innate lymphoid cells (IL-10$^+$ ILC2s) in modulating grass-pollen allergy. We demonstrate that KLRG1$^+$ but not KLRG1$^-$ ILC2 produced IL-10 upon activation with IL-33 and retinoic acid. These cells attenuated Th responses and maintained epithelial cell integrity. IL-10$^+$ KLRG1$^+$ ILC2s were lower in patients with grass-pollen allergy when compared to healthy subjects. In a prospective, double-blind, placebo-controlled trial, we demonstrated that the competence of ILC2 to produce IL-10 was restored in patients who received grass-pollen sublingual immunotherapy. The underpinning mechanisms were associated with the modification of retinol metabolic pathway, cytokine-cytokine receptor interaction, and JAK-STAT signaling pathways in the ILCs. Altogether, our findings underscore the contribution of IL-10$^+$ ILC2s in the disease-modifying effect by allergen immunotherapy.

INTRODUCTION

Seasonal allergic rhinitis (SAR) is an allergen-induced upper airway disease that affects the quality of life of up to 30% adults and 40% children globally. Widely available pharmacotherapies such as antihistamines and corticosteroids can provide only temporary relief in the majority of patients. However, in the few who do not respond to these pharmacotherapies, allergen-specific immunotherapy (AIT) is often indicated (Shamji and Durham, 2017; Canonica et al., 2014; Demoly et al., 2016). AIT is an effective disease-modifying treatment for SAR that can be administered either subcutaneously (SCIT) or sublingually (SLIT). AIT confers long-term clinical benefit following discontinuation of treatment when administered over the course of 3 years (Durham et al., 2010, 1999; Dahl et al., 2006; Durham et al., 2012; Didier et al., 2011, 2015; Ott et al., 2009; Walker et al., 1995; James et al., 2011). The efficacy of SCIT and SLIT is underscored by the induction of tolerance and modification of innate and adaptive immune responses. This includes suppression of type 2 T helper (Th2) cell immunity (Scadding et al., 2015, 2017; Renand et al., 2018), induction of regulatory T cells (Shamji et al., 2019; Bohle et al., 2007; Radulovic et al., 2008; Rolland et al., 2010; Scadding et al., 2010), immune deviation toward Th1 cell responses (Durham et al., 1996; Wachholz et al., 2003), and

induction of interleukin-10 (IL-10)-producing regulatory B cells (Rosser and Mauri, 2015; van de Veen et al., 2013).

The epithelial barrier forms the primary line of defense against microorganisms to ensure host survival and pathogen clearance. Exposure to environmental cues such as allergens including proteases can result in the imbalance of airway epithelial homeostasis, increased production of cytokines, and the subsequent development and exacerbations of type 2 allergic inflammation (Sugita et al., 2018; Schleimer and Berdnikovs, 2017). Epithelial-derived cytokines are key activators of type 2 innate lymphoid cells (ILC2s), which are essential contributors in the pathophysiology of upper airway diseases (Kortekaas Krohn et al., 2018b, 2018a; Lao-Araya et al., 2014).

ILC2s are involved in early stages of the immune host defense mounted against helminths but also contribute to airway inflammation (Golebski et al., 2019; Bal et al., 2016) and allergy (Doherty et al., 2014; Lao-Araya et al., 2014). ILCs in peripheral blood from healthy individuals comprise CRTH2$^+$ ILC2s and CD117$^+$CRTH2$^-$ precursors of mature ILCs (Lim et al., 2017; Nagasawa et al., 2019). A subset of the CD117$^+$ CRTH2$^-$ ILC population expresses the killer cell lectin-like receptor G1 (KLRG1), which is a precursor of ILC2s (Nagasawa et al., 2019). More recently, a subset of ILC2s with the capacity to produce the regulatory cytokine IL-10 has been described (Wang et al., 2017; Seehus et al., 2017; Morita et al., 2019; Bando et al., 2020). Here, we examined whether IL-10-producing regulatory ILCs with immunomodulatory functions play a role in a successful AIT.

RESULTS

ILC2 precursors can differentiate into IL-10-producing ILC2

Recently, we have identified a population of CD117$^+$ ILC2 precursors (Nagasawa et al., 2019). These cells express many hallmarks of ILC2s but lack the mature ILC2 marker CRTH2. Although they are biased to become ILC2, a proportion of KLRG1$^+$CRTH2$^-$ ILCs can acquire the capacity to produce IL-17A, IL-22, and interferon (IFN)-γ when cultured with IL-1β and IL-23 (Nagasawa et al., 2019). The differential gene-expression pattern and functional differentiation capabilities of KLRG1$^+$CRTH2$^-$ ILCs and more mature CRTH2$^+$ ILC2s are likely reflected by differences in their epigenome, as epigenetic priming of gene-regulatory elements is linked to cellular plasticity (Stadhouders et al., 2018). The capacity of these cells to differentiate into IL-10-producing ILCs was, however, not investigated in our previous study. Since recent studies report that a vitamin A metabolite, retinoic acid (RA), is capable of inducing the conversion of mouse and human ILC2 toward IL-10-producing ILCs (Morita et al., 2019; Wang et al., 2017), we analyzed KLRG1$^+$CRTH2$^-$ ILCs cultured with IL-2, IL-7, and IL-33 in the presence or absence of RA. Whereas IL-5 and IL-13 were detected in all activation conditions, only those ILC2s stimulated in the presence of RA produced IL-10 (Figures 1A and 1B). IL-5 production was significantly lower in the presence of RA than in its absence. In addition, a fraction of IL-10$^+$ ILCs co-expressed IL-13 but not IL-5 (Figure S1). These data indicate that induction of IL-10 by RA is accompanied with a reduction of IL-5 expression. GATA-3 transcription factor expression was induced both in the presence and absence of RA (Figures 1C and 1D), which confirmed that IL-10-producing ILCs maintained their phenotype. ILC2s were capable of transdifferentiating into IL-17-producing ILCs (Golebski et al., 2019) or IFN-γ-producing ILCs (Bal et al., 2016) when exposed to IL-2, IL-1β, IL-23, and transforming growth factor β (TGF-β) or IL-2, IL-1β, and IL-12, respectively. However, none of these conditions led to IL-10 production (Figures 1A and 1B).

KLRG1$^+$, but not KLRG1$^-$, ILC2s are capable of producing IL-10

Analyzing the expression of KLRG1 and CRTH2 on peripheral blood CD127$^+$ ILCs, we observed a previously not described subset of CRTH2$^+$ ILCs that lacked KLRG1 (Figure 2A). We exposed four ILC populations (KLRG1$^+$CRTH2$^+$; KLRG1$^-$CRTH2$^+$; the KLRG1$^+$CRTH2$^-$ precursors and KLRG1$^-$CRTH2$^-$) from the peripheral blood to IL-2, IL-7, IL-33, and RA and found that only the KLRG1$^+$ ILC populations produced IL-10, whereas IL-13 production was not restricted to any of these population (Figure 2B). IL-5 was produced by the KLRG1$^+$CRTH2$^+$, KLRG1$^-$CRTH2$^+$ ILCs, and by the KLRG1$^+$CRTH2$^-$ precursors (Figure 2C). The observation that KLRG1$^-$CRTH2$^+$ ILCs produced IL-5 and IL-13 indicated that these cells are ILC2. However, only KLRG1$^+$ cells were able to produce IL-10.

To rule out the possibility that the observed IL-10 production by KLRG1$^+$CRTH2$^+$ ILC2s in response to IL-7, IL-33, and RA was a consequence of a preferential outgrowth of contaminating cells, we generated clones of peripheral blood KLRG1$^+$CRTH2$^+$, KLRG1$^-$CRTH2$^+$, and KLRG1$^+$CRTH2$^-$ ILCs using the OP9-DL1 cell line and IL-2, IL-7, IL-33, and RA. The cloning efficiency was 9%–16%. All clones derived either from KLRG1$^+$ and KLRG1$^-$ CRTH2$^+$ ILCs produced IL-5 and IL-13. Fifty percent of the clones derived from KLRG1$^+$ CRTH2$^-$ ILCs produced IL-10 and 25% substantially produced IL-10. In contrast, only a minor proportion (6%) of the clones derived from KLRG1$^-$CRTH2$^+$ produced IL-10. These data confirm that the capacity to produce IL-10 is restricted to KLRG1$^+$CRTH2$^{+/-}$ cells (Figure 2D). Taken together, these data demonstrate that both KLRG1$^-$ and KLRG1$^+$CRTH2$^+$ ILCs belong to the ILC2 lineage but that IL-10 can only be produced by KLRG1$^+$ ILC2s or their precursors.

We then investigated the expression patterns of genes associated with regulatory functions in IL-10-producing ILC2s. A single-cell Cellular Indexing of Transcriptomes and Epitopes by Sequencing (scCITE-seq) analysis revealed that, following RA stimulation, IL-10$^+$ ILC2s significantly upregulated *CTLA4* and *IL2RA* expression compared to IL-10$^-$KLRG1$^+$ ILCs. *GATA3* and *PTGDR2* genes and CRTH2 protein were not differentially expressed between IL-10$^+$ and IL-10$^-$ ILC2s (Figure 3A). Expression of other T regulatory cell genes such as *FOXP3* could not be detected. Using qRT-PCR, we confirmed the expression of genes encoding molecules that characterize regulatory T (Treg) cells. CTLA4 and IL2RA (CD25) transcripts and protein were enhanced in IL-10-producing KLRG1$^+$ ILC subset as compared to IL-10$^-$ subset (Figures 3B and 3C), whereas *HELIOS*, *BLIMP1*, *CCR4*, *CCR8*, and *IRF4* were the same in IL-10$^+$ and IL-10$^-$ ILC2s (Figure 3B).

We then asked whether IL-10-producing ILCs helped to shape the downstream immune responses in the local tissue environment. To address this, IL-10$^+$ ILCs were co-cultured with CD4$^+$

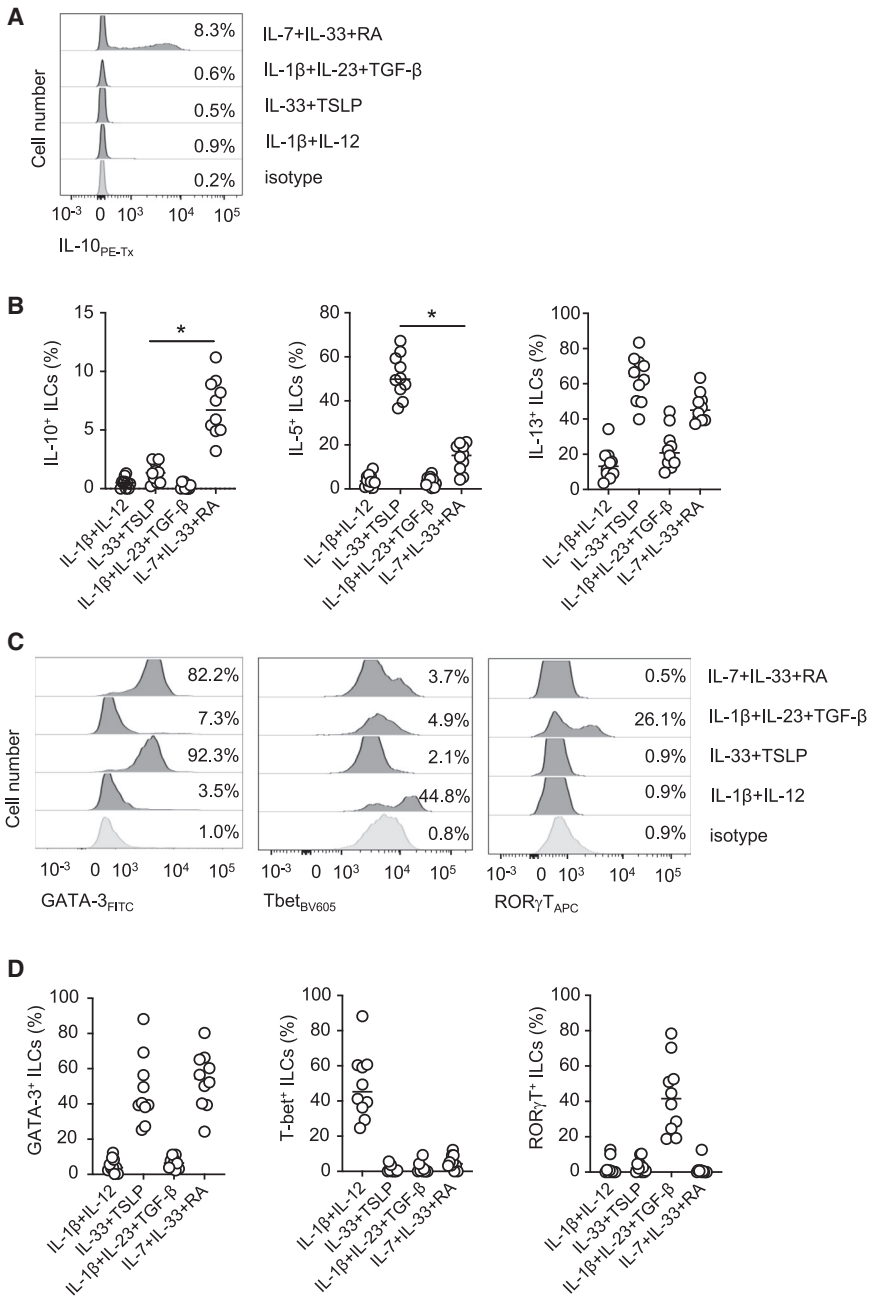

Figure 1. IL-10$^+$ ILCs share characteristics with CRTH2$^+$ ILC2s

Quantification of IL-5, IL-13, and IL-10 production (A and B) and expression of GATA-3, T-bet, and ROR-γT (C and D) by peripheral blood KLRG1$^+$ ILCs that are exposed to activating cytokines for 7 days. Expression and production of cytokines and transcription factor proteins were measured by flow cytometry. Representative histograms (out of ≥7 experiments) of IL-10 (A) and transcription factors (C) expression in KLRG1$^+$ ILCs after culture as in (B) and (D). Each dot represents one individual donor. ILCs from blood of ≥7 donors were analyzed. *p < 0.05 and indicates significant difference between the IL-2, IL-33, TSLP sample, and the marked sample (one-way ANOVA). See also Figure S1.

T cells for 3 days. The activation and proliferation rate of CD4$^+$ T cells was measured. IL-5-producing ILCs significantly increased the Th2 cell responses compared to the IL-2 plus IL-7 expanded ILCs, whereas IL-10$^+$ ILC2s decreased the activation and proliferation of CD4$^+$ IL-4$^+$ T cells. This latter effect was neutralized by anti-IL-10. IL-10$^+$ ILC2s blocked Th1 and Th17 cell responses as well when compared to IL-2 and IL-7 expanded ILCs, and, similarly, this effect was mediated by IL-10. However, IL-5$^+$IL-10$^-$ ILCs also inhibited induction of IFN-γ and IL-17-producing cells when compared to IL-2 and IL-7 expanded ILCs indicating that IL-10$^-$ ILC2 attenuated Th1 and Th17 cell responses as well (Figures 3D–3F). IL-10-producing ILC2s partially prevented phosphorylation of CD28 in T cells, and this effect was diminished by the addition of IL-10-blocking antibody (Figure S2) indicating that IL-10-producing ILC2s affect CD4$^+$ T cell activation and proliferation by inhibiting CD28 signaling (Taylor et al., 2007). Taken together, IL-10-producing ILC2s attenuate all T cell responses in an IL-10-dependent manner, whereas IL-5-producing ILCs stimulate Th2 but attenuate Th1 and Th17 cell responses.

IL-10$^+$ ILC2s regulate the tissue balance in allergy setting

IL-10$^+$ ILC2s are present in other type 2-mediated inflammatory diseases of the airways, i.e., nasal polyp from chronic rhinosinusitis patients (CRSwNP) (Figure S3). We then asked whether IL-10$^+$ ILC2s help to maintain or to restore the nasal epithelial barrier integrity disrupted by an allergen. We found that *IL10R* was expressed in the nasal epithelium after stimulation with environmental triggers including allergens (Figure 4A). Next, we set up cultures of nasal epithelium in the air-liquid interface system (Figure 4B). Fully differentiated epithelium with ciliated and goblet cells was co-cultured for 48 h with ILCs previously polarized toward IL-10 production. This was followed by exposure to grass-pollen allergen (*Phleum pratense*, Phlp) for additional 48 h. We included a sample in which epithelial cells were first exposed to Phlp and subsequently co-cultured with ILCs. The measurements of transepithelial electrical resistance (TEER) demonstrated that Phlp exposure decreased the barrier integrity and that IL-5-producing ILCs amplified the barrier deterioration (Figure 4C). In contrast, co-culture with IL-10-producing ILC2s both prevented the barrier from disintegration or helped restore the epithelial integrity. Addition of IL-10-neutralizing antibody prevented the protective or restoring effect of IL-10. That IL-10 restores disintegration of epithelial cells induced by

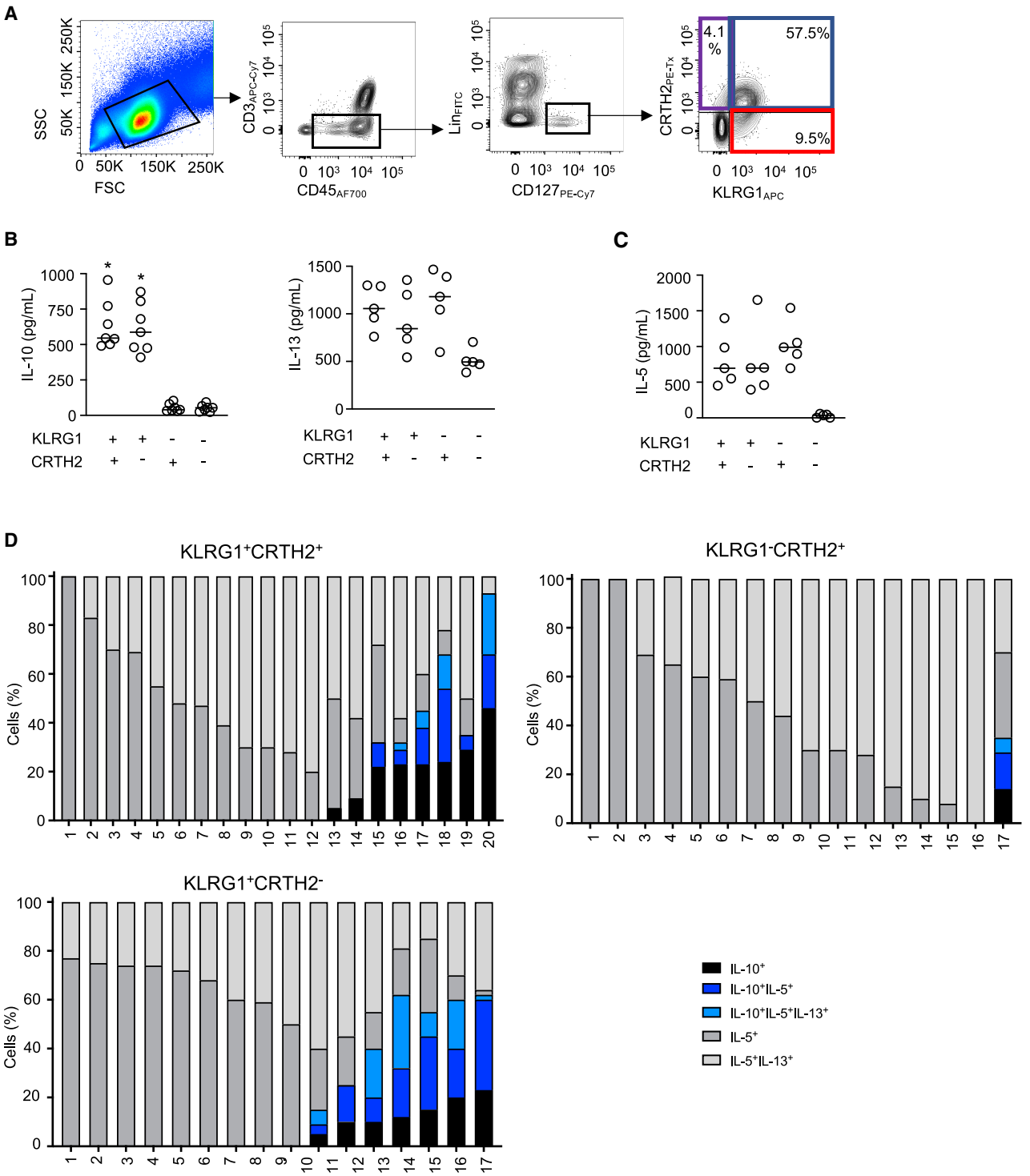

Figure 2. IL-10-producing ILCs are present within KLRG1$^+$ compartment

(A) Flowcytometry gating strategy to identify KLRG1$^+$ ILCs in peripheral blood.

(B and C) IL-10 and IL-13 (B) or IL-5 (C) production by CRTH2$^+$ and/or KLRG1$^+$ CD127$^+$ ILC subpopulation exposed to IL-2, IL-7, IL-33, and RA for 7 days.

(D) KLRG1$^{+/-}$ CRTH2$^{+/-}$ ILCs give rise to IL-10-producing clones after exposing single ILCs from peripheral blood to IL-2, IL-7, IL-33, and RA and subsequently to PMA and ionomycin. Each dot represents one individual donor and $\geq$5 donors were analyzed.

In (B), KLRG1$^+$ versus KLRG1$^-$ ILCs were compared for the statistical significance. *$p < 0.05$ (one-way ANOVA). See also Figure S2.

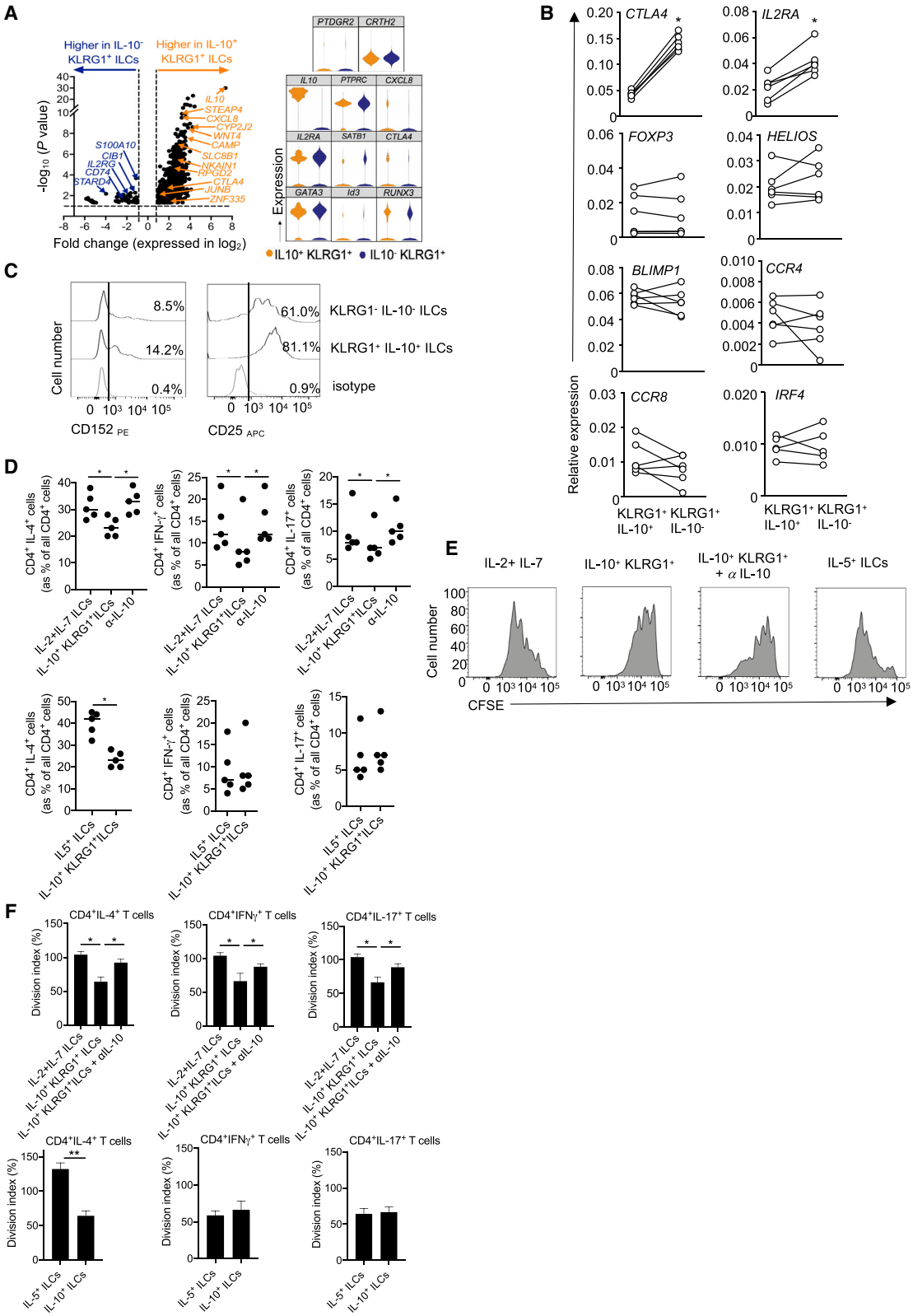

Figure 3. Gene expression by IL-10-producing ILCs

(A) Differential gene expression between IL-10⁺KLRG1⁺ and IL-10⁻KLRG1⁺ cells was performed using scCITE-seq in a total of 10,894 cells of NACs subject following *in vitro* culture for 7 days to IL-2, IL-7, IL-33, and RA. Differential gene-expression analysis was performed using ANOVA.

(legend continued on next page)

allergen was supported by the observation that expression of the tight junction protein zonula occludens-1 (ZO-1) was downregulated by the stimulation with Phlp and restored by IL-10 or IL-10-producing ILCs (Figure 4C). In previous studies (Vroling et al., 2008; Golebski et al., 2015), we demonstrated that epithelium from allergic individuals is in a permanently activated inflammatory state with transcription factors (TFs) from nuclear factor κB (NF-κB) (i.e., p65) and AP-1 (i.e., c-Myc) family being upregulated at the baseline and upon exposure to an allergen as compared to epithelium from healthy volunteers. At the same time, the expression of TFs that are known to inhibit inflammation (i.e., EGR-1) was significantly reduced in epithelium from allergic patients (Vroling et al., 2008; Golebski et al., 2015). This prompted us to investigate the effects of IL-10$^+$ ILC2s on the constitutively activated state of epithelial cells. Figure 4D demonstrates that IL-10-producing ILC2s attenuated in an IL-10-dependent manner the expression of pro-inflammatory genes from the NF-κB family (*NFKB1*) and AP-1 family (*MYC*) in nasal epithelium exposed to the grass-pollen allergen and enhanced the expression of the anti-inflammatory transcription factor *EGR1*, as compared to IL-5-producing ILC2s or epithelium that was not co-cultured with ILCs (Figure 4D). Dysregulated expression of TFs in allergic epithelium may impact the epithelial barrier integrity, as IL-6 and IL-8 were implicated in promoting the epithelial and endothelial barrier permeability (Yu et al., 2013; Al-Sadi et al., 2014). Here, we demonstrated that, in contrast to IL-5-producing ILCs, IL-10$^+$ ILC2s downregulated the production and release of IL-6 and IL-8. This downregulation was, at least partially, mediated by IL-10 (Figure 4E). Finally, we exposed fully differentiated nasal epithelium to Phlp allergen for 24 h in the presence or absence of anti-IL-6 and anti-IL-8 mAbs and measured TEER values. We showed that blocking IL-6 and IL-8 was critical for maintaining the epithelial barrier integrity in this setting (Figure 4F). It should be noted that IL-6 enhanced IL-10 production by ILC2s stimulated by IL-2, IL-7, and IL-33 in the presence of RA (Figure 4G). Thus IL-6 has a Janus face-like role in regulation of epithelial barrier integrity. It enhanced the induction of protective IL-10$^+$ ILC2, and, on the other hand, it should be regulated to prevent compromising the integrity of epithelial cells.

Taken together, these data suggest that IL-10$^+$ ILC2s play a relevant role in maintaining the epithelial barrier integrity upon allergen exposure.

scCITE-seq analysis revealed dysregulation in the type 2 response of ILCs in allergics

ILC2s have previously been implicated as one of the drivers of allergic inflammation. To characterize the impact of seasonal allergy on the composition of ILC and their cytokine profiles, we enumerated the proportions of peripheral-blood-derived ILC subsets in grass-pollen allergics (GPAs) and non-allergic controls (NACs), during the grass-pollen season *ex vivo*. The proportion of ILC2 was significantly higher in GPAs, compared to NACs (Figure 5A; Table S1) consistent with observations in previous studies (Lao-Araya et al., 2014; Doherty et al., 2014). We then determined the expression of cytokines following isolation of the ILCs in GPAs and NACs and observed increased proportions of IL-13$^+$ ILC2s in GPAs but no difference in the proportion of IL-5$^+$ ILC2s. We could not detect IL-10$^+$ cells among the freshly isolated peripheral blood ILC2s neither in GPAs nor in NACs. There were no differences in the proportions of ILC3 and IL-17A$^+$ ILC3s in the peripheral blood between GPAs and NACs during the grass-pollen season (Figure 5A).

To investigate the differential gene-expression profiles between the two patient groups, we interrogated 1,994 and 2,044 ILCs in GPAs and NACs, respectively, and hierarchical analysis was performed to generate a heatmap and volcano plot (Figure 5B). A total of 2,345 genes were differentially expressed (fold changes < -1.5 and >1.5; false discovery rate [FDR] <0.05) and included genes such as *KLRG1*, *KLF2*, *DUSP4*, *JUNB*, *IL2RA*, and *CCL5*. Within the CD127$^+$ ILCs, further classifications of ILC2s and CD117$^+$ ILC precursors, a majority of which are ILC3 precursors (Nagasawa et al., 2019), were performed based on their protein and gene expression (CITE-seq). ILC2s were classified as those that express CRTH2, *PTGDR2*, or *GATA3*, and ILC precursors are those that express CD117 or *KIT*. A total of 1,524 genes and 737 genes were differentially expressed (fold changes < -1.5 and >1.5; FDR <0.05) between GPAs and NACs for ILC2 (Figure 5C) and ILC precursors (Figure 5D), respectively. Single-cell CITE-seq analysis on the overall ILC population illustrated that of the differentially expressed genes between GPAs and NACs; many are related to immune functions such as upregulation of pro-inflammatory chemokines (i.e., *CCL5*, *CCR2*, *CCL3L1*, *CCL3*, *CCR7*, and *CX3CR1*) and cytokine receptors (i.e., *IL5RA*) (Figure 5E). Importantly, genes implicated in retinoic acid synthesis (*DHRS3*) were found upregulated in NACs compared to GPAs. Within the ILC2 population, several genes found differentially expressed between the GPA and NAC group were implicated in cell-differentiation pathway (i.e., *IL2RA* and *Runx3*) (Figure S4). Finally, pathway enrichment analysis on the ILC precursors of GPAs and NACs highlighted differential expression of genes associated with cytokine-cytokine receptor interaction (i.e., *CXCR4* and *IL2RA*) (Figure 5F). Altogether, these data highlight the differential transcriptomic profile in ILCs of GPAs and NACs. These differences support

(B) Expression of Treg cell-related genes within the IL-10$^+$ or IL-10$^-$ KLRG1$^+$ ILC2 population. IL-10$^+$ or IL-10$^-$ KLRG1$^+$ clones were generated after exposing single blood KLRG1$^+$ ILCs to IL-2, IL-7, IL-33, and RA. The expression of Treg cell markers was measured with qPCR. Each dot represents a single clone with matched donors (six clones from three different donors).

(C) Representative (out of ≥3 experiments) histogram plots of expression of CD152 and CD25 in KLRG1$^+$ IL10$^+$ or IL-10$^-$ ILC clones analyzed by flow cytometry.

(D–F) IL-10$^+$ KLRG1$^+$ ILC2s attenuate the activation of CD4$^+$ T cells. (D) IL-10$^+$- or IL-5$^+$- or non-activated ILCs and T cells were co-cultured for 3 days in the presence of IL-2 with or without IL-4. IL-10$^+$ and IL-5$^+$ ILCs were generated by exposing single blood KLRG1$^+$ ILCs to IL-2, IL-7, IL-33, and RA or to IL-2, IL-33, and TSLP. In some conditions, anti-IL-10 blocking mAbs were added. T cells were harvested and intracellular IL-4, IFN-γ, and IL-17 were depicted as a percentage of total CD4$^+$ T cells. *$p < 0.05$ (one-way ANOVA or Student's t test). (E and F) CD4$^+$ cells were labeled with CFSE and co-cultured with ILCs as in (D). The CFSE fluorescence was analyzed by flow cytometry and the division index was calculated.

Representative (out of ≥5 experiments) histograms of CD4$^+$IL-4$^+$ T cells are shown, and summarized data are shown as individual values and mean values ± SEM. *$p < 0.05$ (one-way ANOVA). See also Figure S3.

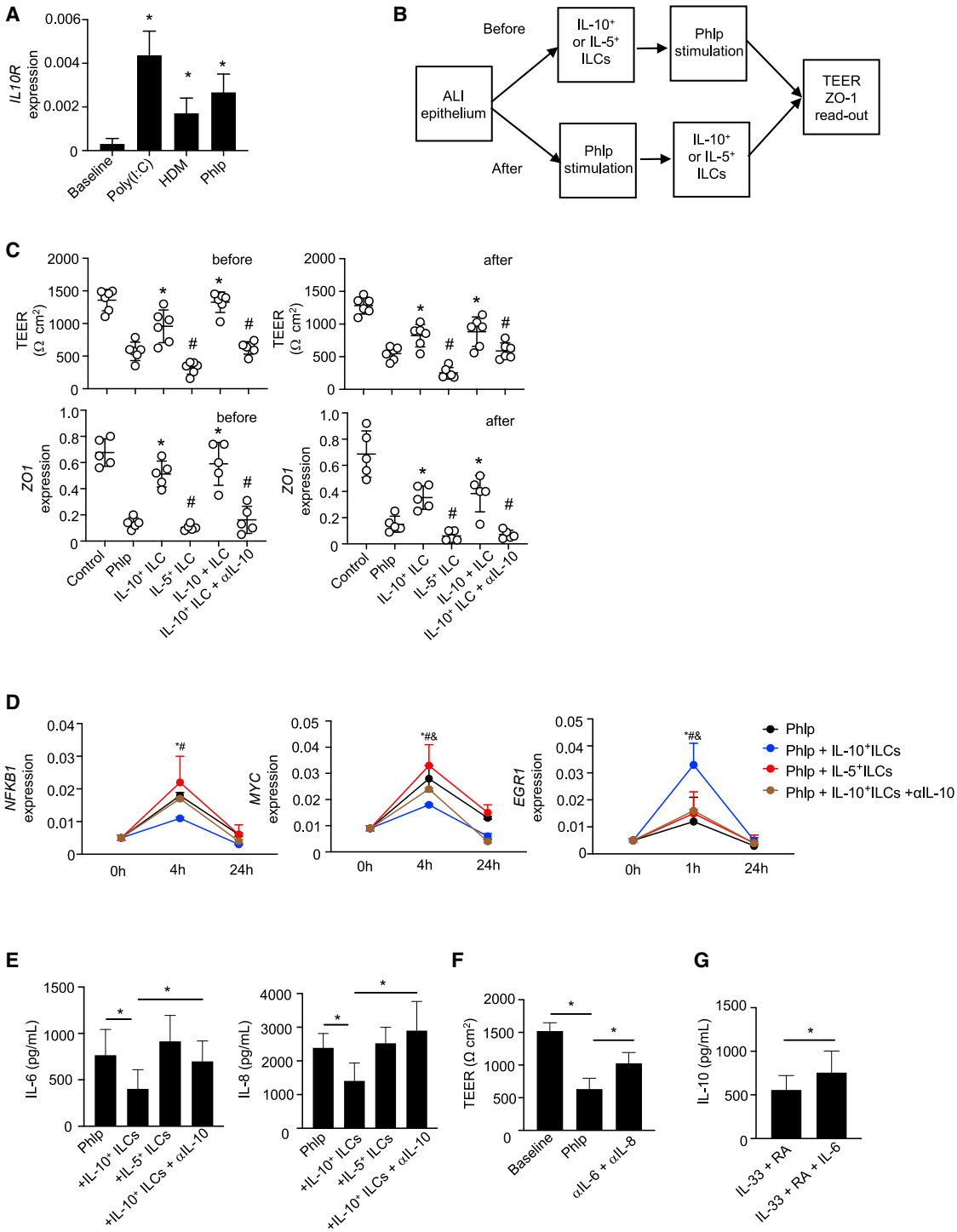

Figure 4. IL-10-producing ILCs reduce type 2 inflammation

(A) Nasal epithelium (n = 3) exposed to poly(I:C), HDM allergen, and Phlp for 24 h. *IL10R* expression was measured by qPCR. Statistical comparison was determined between each stimulus versus control condition.

(B and C) Nasal epithelium was cultured in the air-liquid interface setting until full differentiation and (1) co-cultured with IL5$^+$ or IL-10$^+$ ILCs for 24 h and subsequently exposed to the allergen for 48 h (before), and (2) exposed to the allergen for 24 h and subsequently co-cultured with ILCs for 48 h in the presence of the allergen (after). ILCs were generated as IL-5$^+$ or IL-10$^+$ clones, and, by the time of co-culture, ILCs were actively producing cytokines. Phlp, IL-10, and anti-IL-10 mAbs were added to some samples. (C) Trans-epithelial resistance values or gene expression of *ZO1* were determined. Nasal epithelium from ≥5 NAC donors was used and ILC clones were generated from ≥3 donors. *p < 0.05 refers to a comparison between given sample and an experimental condition with Phlp alone;

(legend continued on next page)

the notion of predominance and dysregulation of a type 2 response in the ILCs of allergic patients, hence the involvement of ILC2 in the pathophysiology of allergic inflammation.

Allergic patients have low frequencies of ILC2s capable of producing IL-10

In a cross-sectional study, we investigated the capacity of peripheral ILCs collected from grass-pollen allergics (GPAs), house dust mite-allergics (HDMAs), and non-atopic healthy controls (NACs) to become IL-10 producers upon IL-2, IL-7, IL-33, and RA stimulation *in vitro* (Table S2). Following IL-2, IL-7, IL-33, and RA stimulation, the proportion of IL-10$^+$ ILC2s and the amounts of secreted IL-10 in the supernatant was significantly lower in GPAs and HDMAs, when compared to NACs (Figures 6A and 6B). These observations were confirmed using an unbiased clustering tool utilizing tSNE algorithm, which revealed that IL-10-producing ILC2s were localized within a small island of cells that expresses KLRG1 but not CRTH2 which indicates that CRTH2 was downregulated by the activation (Figure 6C). Unbiased clustering analysis using FlowSOM also revealed that IL-10-producing ILC2s were detected within a single cluster node (metacluster 8). Quantification of the population abundance within this cluster demonstrated a dysregulation in the GPAs (55.29-fold decrease) and HDMAs (24.19-fold decrease), when compared to NACs (Figures 6D and 6E). A heatmap representing the phenotypes of each metaclusters of the ILC confirmed that metacluster 8 was phenotypically characterized as IL-10$^+$KLRG1$^+$CD161$^+$CD45$^+$ (Figure 6F). There was a strong positive correlation between the proportion of IL-10$^+$ ILC2s and the amount of IL-10 these cells secrete with proportion of KLRG1$^+$ ILC2s (Figure 6G). The proportion of IFN-γ^+ ILCs remained unchanged across the different patient groups (Figure S5A). Moreover, IFN-γ^+ ILCs does not overlap with IL-10$^+$ ILCs, indicating that these latter cells do not produce IFN-γ (Figure S5B).

As IL-10-producing ILC2s were rare in patients with allergic diseases, we investigated whether disease-modifying treatment of allergen immunotherapy leads to the reappearance of these cells. ILCs from allergic patients receiving grass-pollen subcutaneous immunotherapy (GP-SCIT) had a significantly higher proportion of IL-10$^+$ ILC2s and amount of secreted IL-10 compared to untreated GPAs (Figure 6H). FlowSOM analysis confirmed this increase as illustrated by geometric MFI of IL-10 (1.11-fold increase) and population abundance (14.86-fold increase) of metacluster 8 when compared to GPAs (Figure 6I). A small difference in geometric MFI of IL-10 was also detected in metacluster 2, though no change in population abundance was observed (Figure 6I). No IL-10 was detected in any other metaclusters (Figures S6A and S6B). Finally, a strong negative correlation was observed between the capacity of KLRG1$^+$ ILCs to produce IL-10 and clinical symptoms total nasal symptom scores (TNSSs) and visual analog scale (VAS) (Figure 6J).

The observation that the IL-10-producing ILC2 could not be detected in patients with allergic diseases raised the possibility that *in vivo* responses to an allergen challenge are different between healthy controls and allergic individuals. To address this, we challenged NACs and sensitized allergic patients with grass-pollen allergen. Then, we isolated peripheral blood KLRG1$^+$ ILCs and measured the capacity of IL-10 production *in vitro* upon IL-7, IL-33, and RA stimulation. Before the challenge, KLRG1$^+$ ILCs from NACs produced significantly more IL-10 than ILCs from allergic subjects (Figure 6K). The allergen challenge enhanced IL2, IL-7, IL-33, and RA-induced IL-10 production in NACs, while it remained unchanged in allergic individuals (Figure 6K). The nasal epithelium produces IL-33 and TSLP in response to the stimulation with allergens (Golebski et al., 2016). To address whether IL-33 and TSLP were sufficient for inducing IL-10 production by ILC2s once these cells are elicited by allergen challenge *in vivo*, we exposed peripheral blood ILCs obtained from challenged NACs or allergic patients to IL-33 and TSLP for 7 days. ILCs from challenged NACs produced IL-10, whereas ILCs from allergic individuals did not (Figure 6L). No difference in IL-5 production between NACs and allergic patients was found upon ILC stimulation with alarmins (Figure 6L).

Elevated amounts of IL-33 and TSLP are found in nasal secretions of patients with allergic rhinitis (Asaka et al., 2012; Tyurin et al., 2017), and nasal epithelium from individuals with type 2 inflammatory diseases display enhanced capacity toward the production of alarmins as compared with epithelium from healthy controls (Golebski et al., 2016). We reasoned that constitutively increased amounts of alarmins in nasal tissues of allergic individuals may prevent differentiation of naive ILCs toward IL-10-producing ILC2s. To test this idea, we pre-exposed KLRG1$^+$ ILC2s from peripheral blood of healthy non-atopic donors to IL-33 and TSLP for 5 days and subsequently re-stimulated ILC2s with IL-2, IL-7, IL-33, and RA for additional 7 days and measured IL-10 production in supernatants. We observed that once ILCs are activated with IL-33 and TSLP in the absence of RA, they are no longer capable of producing IL-10, even under subsequent exposure to IL-10-polarizing conditions. By contrast, ILCs pre-activated with IL2, IL-7, and IL-33 in the presence of RA continued to produce IL-10 when restimulated in the absence of RA (Figures 6M and 6N). Similarly, IL-10$^+$ clones generated in the presence of RA could produce IL-10 even in the absence of RA (Figure S6C).

#p < 0.05 refers to a comparison between given sample and an experimental condition with IL-10$^+$ ILCs. Data are represented as individual values with mean ± SEM.

(D) Nasal epithelium (n = 3) exposed to grass-pollen allergen in a time course over 24 h in the presence of: IL-10$^+$ or IL-5$^+$ ILCs (obtained through a clonal expansion from a single KLRG1$^+$ ILC), with or without the anti-IL-10 mAb. The expression of *NKFB1*, *MYC*, and *EGR1* was determined by qPCR. *p < 0.05 refers to differences between Phlp versus Phlp + IL-10$^+$ ILC2s; #p < 0.05 refers to differences between Phlp + IL-10$^+$ ILC2s versus Phlp + IL-5$^+$ ILCs; & p < 0.05 refers to differences between Phlp + IL-10$^+$ ILC2s versus Phlp + IL-10$^+$ ILC2s + anti-IL-10.

(E) IL-6 and IL-8 production (pg/mL) measured in a supernatant of the nasal epithelium (n = 3) exposed for 24 h to Phlp co-cultured with IL-10$^+$, IL-5$^+$ ILCs (clonal expansion). *p < 0.05 between given conditions.

(F) TEER values measured in nasal epithelium exposed for 24 h to Phlp with or without IL-6 or IL-8 blocking antibodies. *p < 0.05 between given conditions.

(G) IL-10$^+$ ILC clones expanded with IL-2, IL-7, IL-33, and RA and subsequently exposed to IL-2, IL-7, IL-33, and RA in bulk with or without IL-6 for 6 days. IL-10 was measured in supernatants (n = 3) *p < 0.05 between given conditions. Statistical significance was determined with one-way ANOVA or Student's t test.

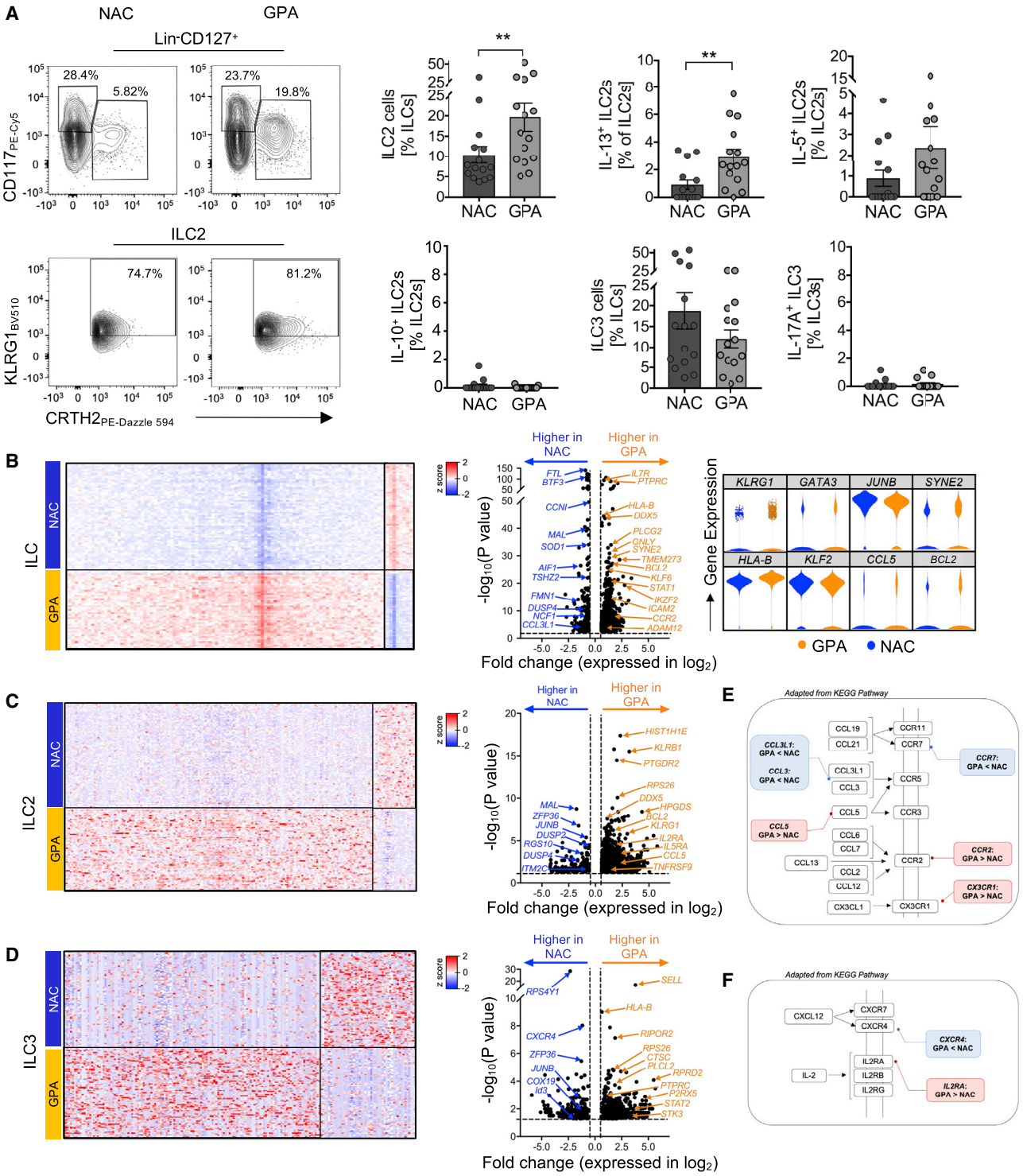

Figure 5. Differential gene expression was observed between ILC subsets of grass-pollen allergics and non-atopic healthy subjects

(A) *Ex vivo* enumeration of the proportion of ILC2, ILC3 and cytokine-producing ILCs in GPAs (n = 15) and NACs (n = 15) during the grass-pollen season. ILCs were defined as cells that are lineage$^-$FcεRI$^-$CD45$^+$CD127$^+$. ILC2 and ILC3 precursor are defined as cells that express CRTH2$^+$CD161$^+$ and CD117$^+$CRTH2$^-$, respectively. Data are represented as mean ± SEM. Statistical significance was determined with Mann-Whitney U test where **p < 0.01.

(B) scCITE-seq was performed *ex vivo* on flow cytometry sorted ILCs from GPA and NAC subjects. Following filtration of contaminating non-ILCs, a total of 2,044 and 1,994 ILCs were analyzed for GPAs and NACs, respectively. Differential gene expression in ILCs of GPAs and NACs were performed using ANOVA and presented as heatmap, volcano plot, and violin plots.

(legend continued on next page)

Taken together, these data indicate that healthy control ILCs exhibit a higher capacity to produce IL-10 than ILCs from allergic individuals. Importantly, alarmins alone induced IL-10 production in peripheral blood ILC2s of NACs once they were challenged with allergen, whereas alarmin-activated peripheral blood ILC2s from challenged allergic patients failed to secrete IL-10. These findings reveal the presence of the downstream tolerogenic innate responses to allergens in non-atopic individuals, which are absent in allergic individuals.

Sublingual allergen-specific immunotherapy induces IL-10$^+$ ILC2s

We investigated the efficacy and molecular mechanisms of grass-pollen sublingual AIT (GP-SLIT) in restoring the frequencies of IL-10$^+$ ILC2s using a combination of *in vitro* cellular assays and scCITE-seq, respectively (Figure 7A; Table S3). GP-SLIT-treated subjects had significantly reduced TNSSs compared to placebo-treated (PL-SLIT) patients after 12 months of treatment but not at the start of treatment (0 m) (Figure 7B). The GP-SLIT-treated patients had increased proportions of IL-10$^+$ ILC2s after 12 and 24 months of treatment when compared to 0 months as determined by intracellular staining with anti-IL-10 antibodies (Figures 7C and 7D) and by the amounts of IL-10 in the supernatant of the stimulated cells (Figure 7E). No changes were observed in the proportion of IL-10$^+$ ILC2s or amounts of secreted IL-10 in PL-SLIT patients after 12 months of treatment when compared to the onset of the treatment (Figures 7D and 7E). These findings were confirmed through the unbiased clustering tools viSNE and FlowSOM. Within the viSNE map, a higher expression of IL-10 and KLRG1 was observed in GP-SLIT patients who have received treatment for 12 and 24 months compared to PL-SLIT (Figure 7F). Previous FlowSOM analysis revealed that IL-10-producing ILCs was found within one single cluster node, metacluster 8, and that this cluster was absent in GPAs (Figure 6D). However, IL-10-producing ILCs were restored following 12 and 24 months of GP-SLIT treatment in metaclusters 8, 2, and 13 (Figure 7G). Further characterization of these metaclusters illustrated that they display the following phenotype: metacluster 2 (KLRG1$^+$CD161$^+$CD45$^+$CRTH2$^+$CD117^{lo} IL-5$^+$IL-13$^+$) and metacluster 13 (IL-10$^+$KLRG1$^+$CD161$^+$CRTH2^{lo}) (Figure 6F). Both the proportion of IL-10$^+$ ILC2s and amounts of secreted IL-10 in GP-SLIT patients after 12 months of treatment negatively correlated with clinical symptoms (Figure 7H). Altogether, these data indicate that SLIT treatment is effective in providing clinical benefit and that this is accompanied by restoration in the capacity of their ILC to produce IL-10.

Single-cell CITE-seq of ILCs was performed to understand the mechanisms of the increased capacity to produce IL-10 following AIT. Analysis of the data demonstrated a differential gene-expression pattern in GP-SLIT 12 and 24 m patients, compared to PL-SLIT 12 m. A total of 7,549, 11,088, and 1,290 cells were investigated for each patient groups, respectively, with a total of 1,181 genes that were differentially expressed (fold change < −1.5 and >1.5; FDR <0.05), which is visualized as a heatmap (Figure 7I). The genes found to be differentially expressed between the different patient groups include not only *IL-10* but also *RDH10*, *DHRS3*, *IL10RA*, *IL10RB*, *JAK1*, *RARA*, *RARG*, *STAT3*, *SOCS1*, and *SOCS3* (Figure 7J). A trend in the induction of *ALDH1A2* was also observed following GP-SLIT. Pathway enrichment analysis demonstrated that these genes are associated with retinol metabolism, cytokine-cytokine receptor interaction, and JAK-STAT signaling pathway (Figure 7K). Collectively, these data suggest that SLIT results in the transcriptional modification in ILCs that drive the production of IL-10 and in parallel, genes implicated in regulating the retinol metabolism.

Consistent with the observation that SLIT induced IL-10-producing ILC2s, the frequencies of peripheral blood-derived ILC2 clones capable of producing IL-10 increased at 6 and 12 m after SLIT. In contrast, in the placebo group at any evaluated time point, only a minor fraction of clones produced IL-10 (Figures S7A–S7C). The IL-10$^+$ clones expressed the ILC2 marker KLRG1, CD45RO, and downregulated the expression of CD62L, while GATA3 expression was the same in all clones confirming that all clones belonged to the ILC2 lineage (Figures S7D and S7E). In this setting, all clones displayed KLRG1 expression, while none of the clones expressed CRTH2 indicating that this receptor either was not expressed on the input cells or was downregulated during the cloning procedure (Figure S7F).

DISCUSSION

Allergen immunotherapy has disease modifying properties by targeting T and B cell responses. Here, we present the evidence that IL-10-producing ILC2s can regulate the pathology of grass-pollen-induced allergy. We demonstrated that the capacity to produce IL-10 is present in KLRG1$^+$ ILC2 precursors and in mature CRTH2$^+$KLRG1$^+$ ILC2s. CRTH2$^+$ILC2s that lack KLRG1 could not be induced to produce IL-10. Those KLRG1$^-$CRTH2$^+$ cells belonged to the ILC2 lineage because they produced IL-5 and IL-13 but not signature cytokines of other ILC subsets. These data indicate that only ILC2 precursors and mature ILC2s that express KLRG1 contained cells that can be induced to produce IL-10.

Like naive T cells, peripheral-blood CD127$^+$CD117$^+$ ILCs express CD45RA and CD62L (Nagasawa et al., 2019). Circulating naive ILC2s may populate the mucosal sites, where, in response to local tissue microenvironment cues that include RA, these cells may differentiate to stable IL-10-producing mature ILC2s. This was supported by our long-term clonal expansion experiments, which demonstrated that, once polarized toward IL-10 production, KLRG1$^+$ ILC2s are capable of producing IL-10 following activation with IL-33 and TSLP in the absence of RA. These findings indicate that IL-2, IL-7, IL-33, and RA may induce maturation of naive ILC2s and ILC2 precursors into IL-10$^+$ KLRG1$^+$ ILC2s and that in mucosal sites these primed ILC2s produce IL-10 in response to alarmins secreted by nasal epithelium

(C and D) ILC2s were classified as those that express CRTH2, *PTGDR2 or GATA3*, and ILC precursors are those that express CD117 or *KIT*. Differential gene-expression analysis between GPAs and NACs in (C) ILC2 and (D) ILC3 are presented as heatmap and volcano plot.
(E and F) Pathway enrichment analyses revealed differential enrichment in genes implicated in cytokine-cytokine receptor interaction for (E) ILC2s and (F) ILC precursors. Cellular pathway diagram is adapted from the KEGG database (path: hsa04060).
See also Figure S4.

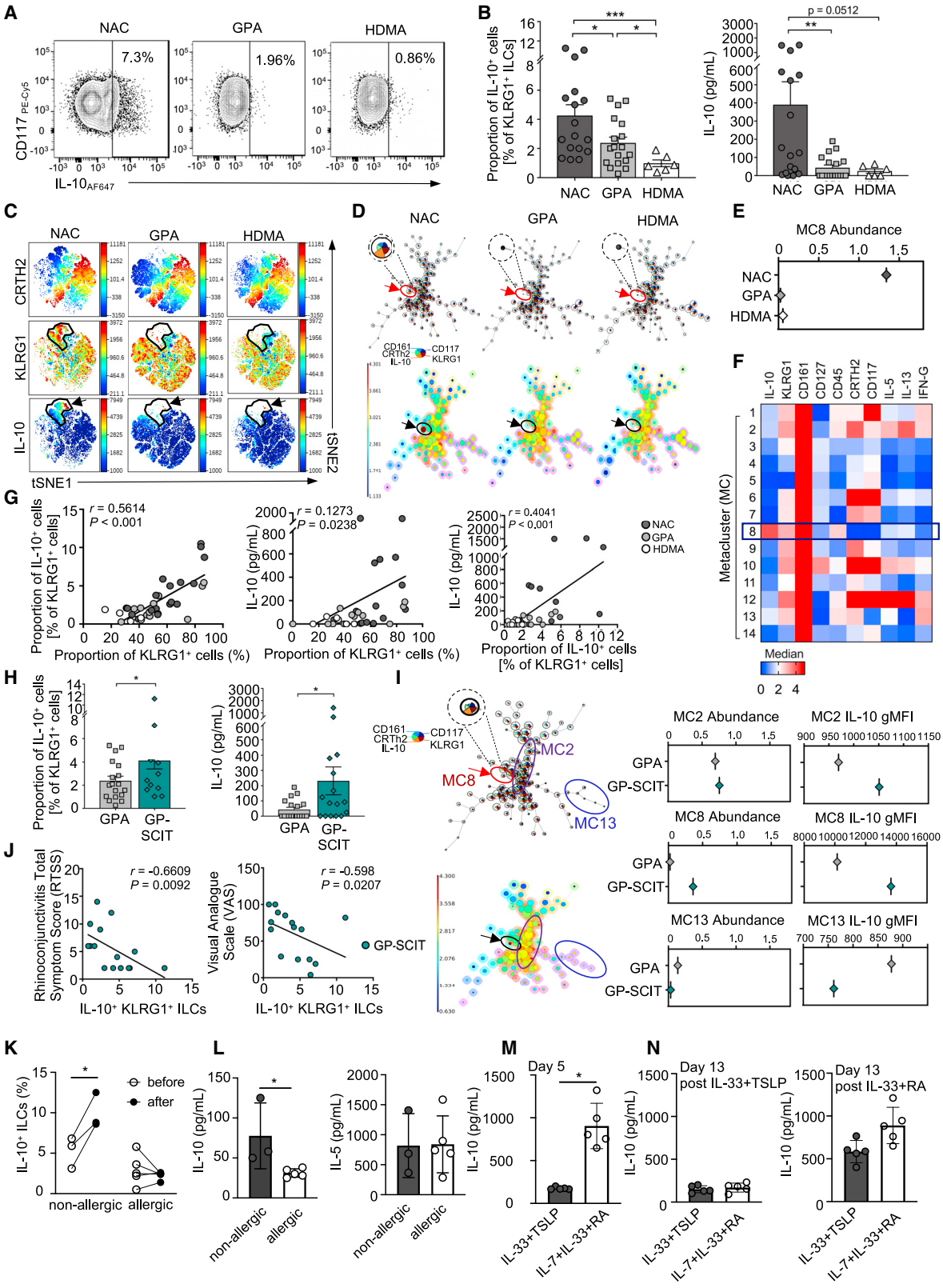

Figure 6. IL-10-producing ILCs are dysregulated in allergic patients

(A) Flow-cytometry representative plots from 6 patients for IL-10^{+}KLRG1^{+} ILCs in NACs (n = 17), GPAs (n = 18), and HDMAs (n = 6).

(B) Induction of IL-10^{+} ILC2s was quantified using flow cytometry and ELISA.

(legend continued on next page)

exposed to an allergen (Golebski et al., 2013; Lambrecht and Hammad, 2014). The observation that peripheral blood KLRG1$^+$ ILC2s from non-allergic individuals challenged with allergen produce IL-10 after stimulation with IL-2, IL-7, and IL-33 in the absence of RA can be explained by assuming that allergen challenge in healthy individuals but not in allergic patients, results in recruitment of ILC2 primed to produce IL-10.

Allergen immunotherapy (AIT) is an effective treatment for upper airway and lower airway disease, such as allergic rhinitis with and without asthma, and confers long-term clinical benefit (Shamji and Durham, 2017). Studies of the mechanisms underlying the clinical response induced by AIT indicate that tolerance is induced and maintained by a complex interplay between the innate, adaptive, and humoral immune response that includes IL-10. Production of IL-10 as a result of AIT has predominantly been associated with the adaptive immune compartment, particularly Treg cells (Bohle et al., 2007; Rolland et al., 2010; Scadding et al., 2010) and Bregs (Rosser and Mauri, 2015; van de Veen et al., 2013, 2016). Our data add ILC2 that can produce IL-10 to the repertoire of immune cells associated with a successful AIT. Grass-pollen SCIT treatment has been shown to suppress seasonal increases of ILC2s (Lao-Araya et al., 2014; Lombardi et al., 2016). Similarly, a recent study of HDM SCIT demonstrates a reduction in the proportion of ILC2s in allergic individuals who respond to treatment compared to untreated allergics (Mitthamsiri et al., 2018). In this study, we report that both grass-pollen SCIT and SLIT induced ILC2s that could produce IL-10 following *in vitro* stimulation with IL-2, IL-7, IL-33, and RA. These cells may, therefore, contribute to the reduction of ILC2 in allergic individuals treated with AIT. We demonstrated that grass-pollen AIT was able to restore numbers of IL-10-producing ILCs close to those in healthy controls. Using an unbiased machine learning approach, we confirmed that SCIT and SLIT promoted the induction of IL-10-producing ILC2s. Following SCIT treatment, we found IL-10$^+$ ILCs among KLRG1$^+$CD161$^+$ ILC2s that did not express IL-5 and IL-13 and ILC2 that co-expressed IL-5 and IL-13. Our observations that IL-10$^+$ KLRG1$^+$ILC2s are restored in allergic individuals receiving SCIT or SLIT and that the frequencies of IL-10$^+$ ILC2s strongly correlated with improvement in clinical symptoms suggest their potential relevance as a biomarker of AIT efficacy and patient responsiveness.

Pathway enrichment analyses of genes expressed in ILCs revealed that SLIT induces, next to IL-10, several genes implicated in the retinol metabolism pathway (*RDH10*, *DHRS3*, *ALDH1A2*, *RARA*, and *RARG*), cytokine-cytokine receptor pathway (*IL10RA* and *IL10RA*), and JAK-STAT pathway (*JAK1*, *STAT3*, *SOCS1*, and *SOCS3*). Previous studies have already demonstrated that a successful AIT has been associated with induction of *IL10* mRNA expression (Nouri-Aria et al., 2004), but an association with the induction of genes involved in retinol metabolism pathway was not observed before. The induction of IL-10 and its binding to IL10R mediated downstream signaling pathways that included *JAK1* and *STAT3* activation, resulting in *SOCS3* activation, subsequently leading to anti-inflammatory activity. RA has been described as a negative regulator of inflammatory response. Previous studies have demonstrated that T cell stimulated by RA preferentially express RARα and that a pan-RAR antagonist strongly inhibited inducible Treg cell generation making them a central receptor that mediates the function of RA (Coombes et al., 2007; Mucida et al., 2007; Sun et al., 2007). Our findings demonstrate that GP-SLIT can result in the induction of *RARA* gene in a time-dependent manner, which may be important for the downstream action of RA. It has been documented that RA signaling is crucial for the development of oral tolerance since RA-mediated trafficking of T cells was required for a sustained expansion of inducible Treg cell numbers in the gut, which is achieved through IL-10-mediated interactions with resident antigen-presenting cells (Hadis et al., 2011). However, the mechanism by which SLIT results in enhanced retinol metabolism in ILCs remains to be fully identified. Further studies to investigate the epigenetic features at the *IL-10* locus is warranted and would provide more insight into the molecular mechanism.

One mechanism by which IL-10$^+$ ILC2s regulate allergic reactions is by preventing the epithelial damage by reducing the production and release of pro-inflammatory epithelial mediators, i.e., IL-6 and IL-8. IL-6 treatment *in vitro* also increases permeability across endothelial cells mediated by the protein kinase C pathway (Desai et al., 2002) and indirect regulation of claudin genes. IL-8 in the intestinal epithelium is sufficient to trigger neutrophil recruitment to the lamina propria via increased permeability of epithelial cells (Kucharzik et al., 2005; Yu et al., 2013). Together our data suggest that IL-10$^+$ ILC2s are involved in maintaining the epithelial barrier integrity upon allergen exposure. Another mechanism of regulation of allergic reactions by IL-10$^+$ ILC2s might be attenuation of Th2 cell responses. We observed that IL-5$^+$IL-10$^-$ ILCs promoted Th2 cell responses *in vitro*, presumably by production of IL-4, whereas IL-10-producing ILCs inhibited Th2 cell responses in an IL-10-dependent way. The inhibition may be attributed to an IL-10-induced blocking of the signal transduction mediated via CD28. IL-10 also increases granzyme B expression in Th2 cells, which may result

(C–E) Unbiased clustering analyses were performed using viSNE (C) and FlowSOM (D and E) to identify clusters of cells that expresses IL-10. Red and blue indicates high and low expression of the indicated marker, respectively.
(F) Heatmap representing phenotype of each ILC metaclusters analyzed by FlowSOM.
(G) Spearman correlation shows a positive association between the proportion of KLRG1$^+$ ILCs and IL-10$^+$ ILC2s or amounts of secreted IL-10.
(H and I) Induction of IL-10$^+$ ILC2s measured through flow cytometry and ELISA in GP-SCIT (n = 15) patients and FlowSOM (I).
(J) Spearman correlation between proportion of IL-10$^+$ ILC2s and clinical symptom scores (RTSS and VAS).
(K) IL-10$^+$ ILC2s from NACs (n = 3) or allergic patients (n = 5) challenged with grass-pollen allergen. ILCs were isolated from peripheral blood and exposed to IL-2, IL-33, and TSLP for 7 days, followed by 3h PMA/ionomycin stimulation and intracellular expression of IL-10 was measured by flow cytometry.
(L) IL-10 and IL-5 amounts in supernatants of KLRG1$^+$ ILCs obtained from the blood of NACs (n = 3) and allergic individuals (n = 5). ILCs were exposed to IL-2, 33, TSLP for 7 days.
(M and N) KLRG1$^+$ ILCs from peripheral blood of NACs (n = 5) were exposed to IL-2, IL-33, and TSLP (mix 1) or IL-2, IL-7, IL-33, and RA (mix 2) for 5 days (M). 7-day exposure to mix 1 or mix 2 of ILCs pre-exposed to mix 1 or mix 2 was followed by measurements of IL-5 and IL-10 in supernatants.
Data are represented as individual values with mean ± SEM. *$p < 0.05$ (one-way ANOVA). See also Figures S5 and S6.

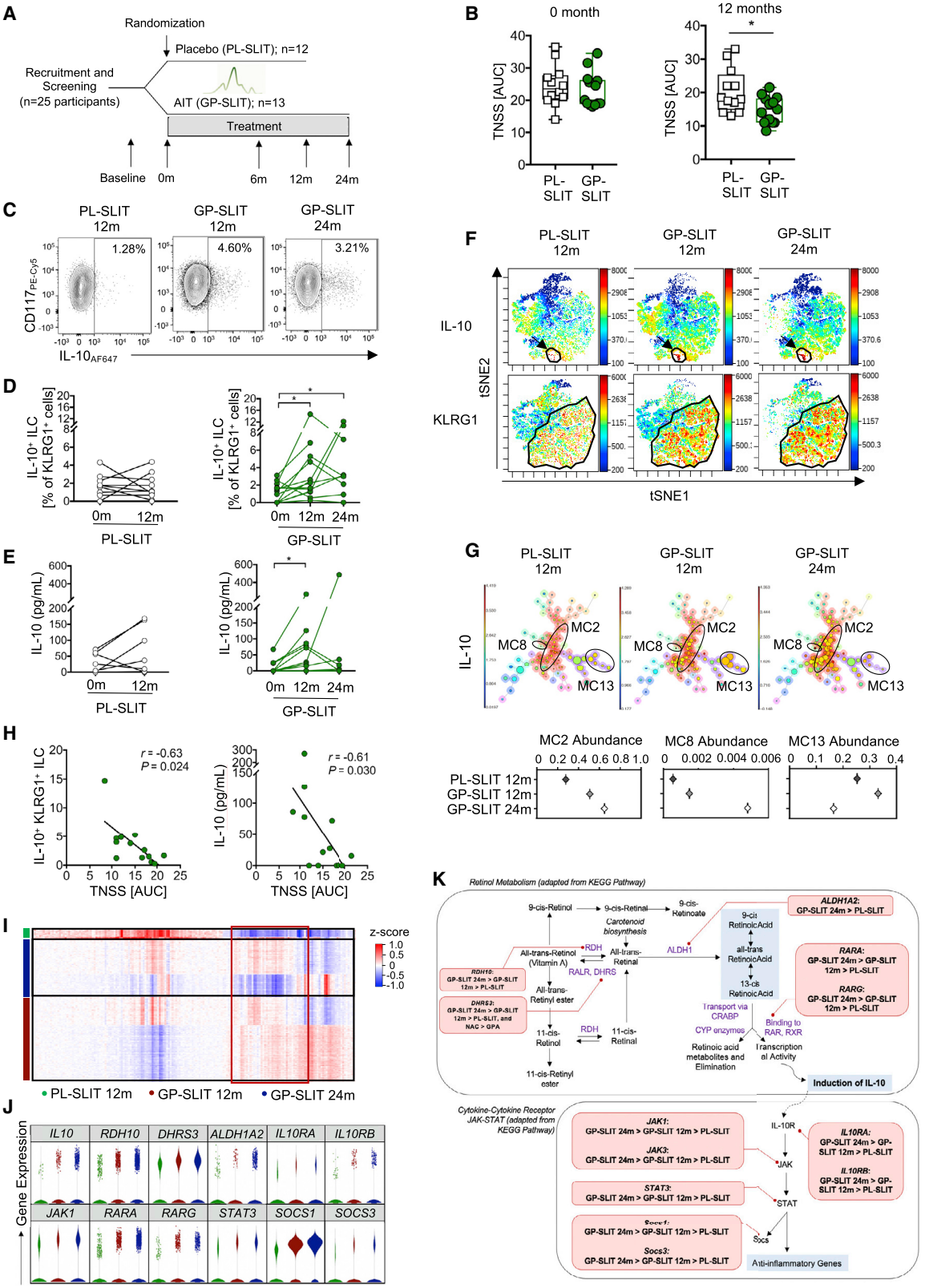

Figure 7. Grass-pollen sublingual allergen immunotherapy can result in the induction of IL-10-producing ILC2s

(A) Study design of the randomized, double-blind, placebo-controlled SLIT trial. Patients either receive placebo (PL-SLIT, n = 12) or active treatment (GP-SLIT, n = 13). Whole-blood samples were collected at various time points indicated by the arrows.

(legend continued on next page)

in increased sensitivity to cell death (Coomes et al., 2017). Thus, the shift in the balance between IL-10$^+$ and IL-10$^-$ ILC2 that produce high amounts of IL-5 may determine the strength of the activation of Th2 cells at mucosal sites.

In conclusion, we show that the frequencies of ILC2s capable of producing IL-10 are closely associated with clinical scores. The increased frequencies of IL-10-producing ILC2s are likely achieved through transcriptional modification of the retinol metabolism, cytokine-cytokine receptor interaction, and JAK-STAT signaling pathways. These IL-10$^+$ ILC2s can repair and maintain epithelial barrier integrity and may control Th cell responses. This study warrants further investigations to validate the use of IL-10-producing ILCs as a biomarker of AIT response.

Limitations of study

We report that peripheral blood KLRG1$^+$ ILC2s have the capacity to produce IL-10 when stimulated with IL-7, IL-33, and RA for 9 days. Moreover, it is well-established that IL-10 production by ILC2s can only occur following *in vitro* stimulation. Studies have shown that naive CD4$^+$ T cells can differentiate into IL-10-secreting T regulatory cells in response to repeated T cell receptor stimulation with anti-CD3 and anti-CD28 followed by PMA and ionomycin stimulation (Groux et al., 1997). In another cell system, IL-10 production by regulatory B cells have also been reported only following stimulation with TLR9 agonist (CpG ODN 2006) and CD40 ligand (CD40L) (Sharif et al., 2019)(Mielle et al., 2018). In line with these studies, production of IL-10 by peripheral blood ILCs also requires *in vitro* stimulation with cytokines. The capacity of ILCs to produce IL-10 may be activated once ILCs are recruited to the airway tissues and exposed to cytokines from the local tissue microenvironment.

STAR★METHODS

Detailed methods are provided in the online version of this paper and include the following:

SUPPLEMENTAL INFORMATION

Supplemental Information can be found online at https://doi.org/10.1016/j.immuni.2020.12.013.

ACKNOWLEDGMENTS

We would like to acknowledge Jane Srivastava and Radhika Patel for help with cell sorting, Susanne Reinartz for help with experimental design, Danielle van Egmond, Esther de Groot, and Maryse Tempert for samples acquisition and experimental work, and colleagues from flow cytometry core facility Amsterdam UMC for help with flow cytometry. The Imperial BRC Genomics Facility provided resources and support that contributed to results reported within this paper. This study was supported by the Imperial College Trust and the NIHR Imperial Biomedical Research Centre. H.S. was supported by an advanced grant of the ERC, #341038. F.Q.H, O.H., M.O., and G.M. were supported by Luxembourg National Research Fund (FNR) grants AFR-RIKEN/11228353/TregBAR (F.Q.H. and M.O.), PRIDE/11012546/NEXTIMMUNE (G.M., F.Q.H., and M.O.), and PRIDE/10907093/CRITICS (F.Q.H.).

AUTHOR CONTRIBUTIONS

Conceptualization, K.G., J.A.L., and M.H.S.; Investigation, K.G., J.A.L., U.S., M.L.-A., R.C.Y.L., S.M.B., and M.L.A.; Resources, E.H.S.-K., G.V.-N., O.F., C.M.v.D., W.J.F., S.R.D., S.J.H.V., and A.-H.M.v.d.Z.; Bioinformatic Analysis, B.A.H., O.H., G.M., F.Q.H., and M.O.; Analysis and Manuscript Writing, K.G., J.A.L., H.S., and M.H.S. All authors critically read the manuscript.

DECLARATION OF INTERESTS

K.G., J.A.L., U.S., M.M.L., R.C.Y.L., S.M.B., B.A.H., G.V.-N., O.H., G.M., F.Q.H., O.F., M.L.A., S.J.H.V., A.-H.M.v.d.Z., C.M.v.D., and W.F. report no conflicts of interest. E.H.S.-K. has received travel grants from ALK-Abello. Stephen Durham has received lecture fees and research funds from ALK, Denmark, manufacturer of grass allergen tablets used for sublingual

(B) Area under the curve (AUC) of total nasal symptom score (TNSS) at 0 and 12 months.
(C) Flow-cytometry representative plots from 6 patients showing IL-10-producing ILC2s in PL-SLIT (12 m) and GP-SLIT (12 and 24 m).
(D–G) Induction of IL-10$^+$KLRG1$^+$ ILCs *in vitro* were quantified using flow cytometry (D) and ELISA (E). Unbiased clustering analyses were performed using viSNE (F) and FlowSOM (G) to identify clusters of cells that expresses IL-10. Red and blue indicates high and low expression of the indicated marker, respectively.
(H) Spearman correlation between proportion of IL-10$^+$ ILC2s, amount of IL-10, and clinical symptom scores (TNSS) in GP-SLIT 12 m patients.
(I) scCITE-seq was performed on flow-cytometry-sorted ILCs of PL-SLIT 12 m (green), GP-SLIT 12 m (red), and GP-SLIT 24 m (blue) following *in vitro* culture with IL-2, IL-7, IL-33, and RA for 7 days. scRNA-seq data were filtered out of any contaminating non-ILCs and a total of 1,290, 7,549, and 11,088 ILCs were analyzed for PL-SLIT 12 m, GP-SLIT 12 m, and GP-SLIT 24 m, respectively. Differential gene expression was performed using ANOVA and presented as a heatmap.
(J) Selected few genes found differentially expressed between the study groups that belong in the red highlighted box in (I).
(K) Pathway enrichment analyses revealed differential expression of genes implicated in the retinol metabolism pathway, cytokine-cytokine receptor interaction, and JAK-STAT signaling pathway. The cellular pathway diagram is adapted from the KEGG database (path: hsa00830, hsa04060, and hsa04630). Data are represented as mean ± SEM. All statistical significance was determined with Mann-Whitney U test where *$p < 0.05$, except for scCITE-seq data in which ANOVA were used. See also Figure S7.

immunotherapy. M.O. is a consultant for Hycor Biomedical and a co-founder of Tolerogenics SARL. Unrelated intellectual property of M.O. and the Luxembourg Institute of Health has been licensed to Tolerogenics. H.S. is a consultant for GSK for which he receives an honorarium. M.H.S. reports research grants from Immune Tolerance Network, Medical Research Council, Allergy Therapeutics, and LETI Laboratorios and lecture fees from Allergy Therapeutics and ALK.

Received: May 7, 2020
Revised: November 4, 2020
Accepted: December 17, 2020
Published: January 14, 2021

REFERENCES

Al-Sadi, R., Ye, D., Boivin, M., Guo, S., Hashimi, M., Ereifej, L., and Ma, T.Y. (2014). Interleukin-6 modulation of intestinal epithelial tight junction permeability is mediated by JNK pathway activation of claudin-2 gene. PLoS ONE *9*, e85345.

Asaka, D., Yoshikawa, M., Nakayama, T., Yoshimura, T., Moriyama, H., and Otori, N. (2012). Elevated levels of interleukin-33 in the nasal secretions of patients with allergic rhinitis. Int. Arch. Allergy Immunol. *158* (*Suppl 1*), 47–50.

Bal, S.M., Bernink, J.H., Nagasawa, M., Groot, J., Shikhagaie, M.M., Golebski, K., van Drunen, C.M., Lutter, R., Jonkers, R.E., Hombrink, P., et al. (2016). IL-1β, IL-4 and IL-12 control the fate of group 2 innate lymphoid cells in human airway inflammation in the lungs. Nat. Immunol. *17*, 636–645.

Bando, J.K., Gilfillan, S., Di Luccia, B., Fachi, J.L., Sécca, C., Cella, M., and Colonna, M. (2020). ILC2s are the predominant source of intestinal ILC-derived IL-10. J. Exp. Med. *217*, e20191520.

Bohle, B., Kinaciyan, T., Gerstmayr, M., Radakovics, A., Jahn-Schmid, B., and Ebner, C. (2007). Sublingual immunotherapy induces IL-10-producing T regulatory cells, allergen-specific T-cell tolerance, and immune deviation. J. Allergy Clin. Immunol. *120*, 707–713.

Canonica, G.W., Cox, L., Pawankar, R., Baena-Cagnani, C.E., Blaiss, M., Bonini, S., Bousquet, J., Calderón, M., Compalati, E., Durham, S.R., et al. (2014). Sublingual immunotherapy: World Allergy Organization position paper 2013 update. World Allergy Organ. J. *7*, 6.

Coombes, J.L., Siddiqui, K.R., Arancibia-Cárcamo, C.V., Hall, J., Sun, C.M., Belkaid, Y., and Powrie, F. (2007). A functionally specialized population of mucosal CD103+ DCs induces Foxp3+ regulatory T cells via a TGF-beta and retinoic acid-dependent mechanism. J. Exp. Med. *204*, 1757–1764.

Coomes, S.M., Kannan, Y., Pelly, V.S., Entwistle, L.J., Guidi, R., Perez-Lloret, J., Nikolov, N., Müller, W., and Wilson, M.S. (2017). $CD4^+$ Th2 cells are directly regulated by IL-10 during allergic airway inflammation. Mucosal Immunol. *10*, 150–161.

Dahl, R., Kapp, A., Colombo, G., de Monchy, J.G., Rak, S., Emminger, W., Rivas, M.F., Ribel, M., and Durham, S.R. (2006). Efficacy and safety of sublingual immunotherapy with grass allergen tablets for seasonal allergic rhinoconjunctivitis. J. Allergy Clin. Immunol. *118*, 434–440.

Demoly, P., Passalacqua, G., Pfaar, O., Sastre, J., and Wahn, U. (2016). Management of the polyallergic patient with allergy immunotherapy: a practice-based approach. Allergy Asthma Clin. Immunol. *12*, 2.

Desai, T.R., Leeper, N.J., Hynes, K.L., and Gewertz, B.L. (2002). Interleukin-6 causes endothelial barrier dysfunction via the protein kinase C pathway. J. Surg. Res. *104*, 118–123.

Didier, A., Malling, H.J., Worm, M., Horak, F., and Sussman, G.L. (2015). Prolonged efficacy of the 300IR 5-grass pollen tablet up to 2 years after treatment cessation, as measured by a recommended daily combined score. Clin. Transl. Allergy *5*, 12.

Didier, A., Worm, M., Horak, F., Sussman, G., de Beaumont, O., Le Gall, M., Melac, M., and Malling, H.J. (2011). Sustained 3-year efficacy of pre- and co-seasonal 5-grass-pollen sublingual immunotherapy tablets in patients with grass pollen-induced rhinoconjunctivitis. J. Allergy Clin. Immunol. *128*, 559–566.

Doherty, T.A., Scott, D., Walford, H.H., Khorram, N., Lund, S., Baum, R., Chang, J., Rosenthal, P., Beppu, A., Miller, M., and Broide, D.H. (2014). Allergen challenge in allergic rhinitis rapidly induces increased peripheral blood type 2 innate lymphoid cells that express CD84. J. Allergy Clin. Immunol. *133*, 1203–1205.

Durham, S.R., Emminger, W., Kapp, A., Colombo, G., De Monchy, J.G., Rak, S., Scadding, G.K., Andersen, J.S., Riis, B., and Dahl, R. (2010). Long-term clinical efficacy in grass pollen-induced rhinoconjunctivitis after treatment with SQ-standardized grass allergy immunotherapy tablet. J. Allergy Clin. Immunol. *125*, 131–138.

Durham, S.R., Emminger, W., Kapp, A., de Monchy, J.G., Rak, S., Scadding, G.K., Wurtzen, P.A., Andersen, J.S., Tholstrup, B., Riis, B., and Dahl, R. (2012). SQ-standardized sublingual grass immunotherapy: confirmation of disease modification 2 years after 3 years of treatment in a randomized trial. J. Allergy Clin. Immunol. *129*, 717–725.

Durham, S.R., Walker, S.M., Varga, E.M., Jacobson, M.R., O'Brien, F., Noble, W., Till, S.J., Hamid, Q.A., and Nouri-Aria, K.T. (1999). Long-term clinical efficacy of grass-pollen immunotherapy. N. Engl. J. Med. *341*, 468–475.

Durham, S.R., Ying, S., Varney, V.A., Jacobson, M.R., Sudderick, R.M., Mackay, I.S., Kay, A.B., and Hamid, Q.A. (1996). Grass pollen immunotherapy inhibits allergen-induced infiltration of CD4+ T lymphocytes and eosinophils in the nasal mucosa and increases the number of cells expressing messenger RNA for interferon-gamma. J. Allergy Clin. Immunol. *97*, 1356–1365.

Golebski, K., Ros, X.R., Nagasawa, M., van Tol, S., Heesters, B.A., Aglmous, H., Kradolfer, C.M.A., Shikhagaie, M.M., Seys, S., Hellings, P.W., et al. (2019). IL-1β, IL-23, and TGF-β drive plasticity of human ILC2s towards IL-17-producing ILCs in nasal inflammation. Nat. Commun. *10*, 2162.

Golebski, K., Röschmann, K.I., Toppila-Salmi, S., Hammad, H., Lambrecht, B.N., Renkonen, R., Fokkens, W.J., and van Drunen, C.M. (2013). The multifaceted role of allergen exposure to the local airway mucosa. Allergy *68*, 152–160.

Golebski, K., van Egmond, D., de Groot, E.J., Roschmann, K.I., Fokkens, W.J., and van Drunen, C.M. (2015). EGR-1 and DUSP-1 are important negative regulators of pro-allergic responses in airway epithelium. Mol. Immunol. *65*, 43–50.

Golebski, K., van Tongeren, J., van Egmond, D., de Groot, E.J., Fokkens, W.J., and van Drunen, C.M. (2016). Specific Induction of TSLP by the Viral RNA Analogue Poly(I:C) in Primary Epithelial Cells Derived from Nasal Polyps. PLoS ONE *11*, e0152808.

Groux, H., O'Garra, A., Bigler, M., Rouleau, M., Antonenko, S., De Vries, J.E., and Roncarolo, M.G. (1997). A CD4+ T-cell subset inhibits antigen-specific T-cell responses and prevents colitis. Nature *389*, 737–742.

Hadis, U., Wahl, B., Schulz, O., Hardtke-Wolenski, M., Schippers, A., Wagner, N., Müller, W., Sparwasser, T., Förster, R., and Pabst, O. (2011). Intestinal tolerance requires gut homing and expansion of FoxP3+ regulatory T cells in the lamina propria. Immunity *34*, 237–246.

James, L.K., Shamji, M.H., Walker, S.M., Wilson, D.R., Wachholz, P.A., Francis, J.N., Jacobson, M.R., Kimber, I., Till, S.J., and Durham, S.R. (2011). Long-term tolerance after allergen immunotherapy is accompanied by selective persistence of blocking antibodies. J. Allergy Clin. Immunol. *127*, 509–516.

Kortekaas Krohn, I., Bal, S.M., and Golebski, K. (2018a). The role of innate lymphoid cells in airway inflammation: evolving paradigms. Curr. Opin. Pulm. Med. *24*, 11–17.

Kortekaas Krohn, I., Shikhagaie, M.M., Golebski, K., Bernink, J.H., Breynaert, C., Creyns, B., Diamant, Z., Fokkens, W.J., Gevaert, P., Hellings, P., et al. (2018b). Emerging roles of innate lymphoid cells in inflammatory diseases: Clinical implications. Allergy *73*, 837–850.

Kucharzik, T., Hudson, J.T., 3rd, Lügering, A., Abbas, J.A., Bettini, M., Lake, J.G., Evans, M.E., Ziegler, T.R., Merlin, D., Madara, J.L., and Williams, I.R. (2005). Acute induction of human IL-8 production by

intestinal epithelium triggers neutrophil infiltration without mucosal injury. Gut *54*, 1565–1572.

Lambrecht, B.N., and Hammad, H. (2014). Allergens and the airway epithelium response: gateway to allergic sensitization. J. Allergy Clin. Immunol. *134*, 499–507.

Lao-Araya, M., Steveling, E., Scadding, G.W., Durham, S.R., and Shamji, M.H. (2014). Seasonal increases in peripheral innate lymphoid type 2 cells are inhibited by subcutaneous grass pollen immunotherapy. J. Allergy Clin. Immunol. *134*, 1193, 5.e4.

Lim, A.I., Li, Y., Lopez-Lastra, S., Stadhouders, R., Paul, F., Casrouge, A., Serafini, N., Puel, A., Bustamante, J., Surace, L., et al. (2017). Systemic Human ILC Precursors Provide a Substrate for Tissue ILC Differentiation. Cell *168*, 1086–1100.e10.

Lombardi, V., Beuraud, C., Neukirch, C., Moussu, H., Morizur, L., Horiot, S., Luce, S., Wambre, E., Linsley, P., Chollet-Martin, S., et al. (2016). Circulating innate lymphoid cells are differentially regulated in allergic and nonallergic subjects. J. Allergy Clin. Immunol. *138*, 305–308.

Mielle, J., Audo, R., Hahne, M., Macia, L., Combe, B., Morel, J., and Daien, C. (2018). IL-10 Producing B Cells Ability to Induce Regulatory T Cells Is Maintained in Rheumatoid Arthritis. Front. Immunol. *9*, 961.

Mitthamsiri, W., Pradubpongsa, P., Sangasapaviliya, A., and Boonpiyathad, T. (2018). Decreased CRTH2 Expression and Response to Allergen Re-stimulation on Innate Lymphoid Cells in Patients With Allergen-Specific Immunotherapy. Allergy Asthma Immunol. Res. *10*, 662–674.

Morita, H., Kubo, T., Rückert, B., Ravindran, A., Soyka, M.B., Rinaldi, A.O., Sugita, K., Wawrzyniak, M., Wawrzyniak, P., Motomura, K., et al. (2019). Induction of human regulatory innate lymphoid cells from group 2 innate lymphoid cells by retinoic acid. J. Allergy Clin. Immunol. *143*, 2190–2201.e9.

Mucida, D., Park, Y., Kim, G., Turovskaya, O., Scott, I., Kronenberg, M., and Cheroutre, H. (2007). Reciprocal TH17 and regulatory T cell differentiation mediated by retinoic acid. Science *317*, 256–260.

Nagasawa, M., Heesters, B.A., Kradolfer, C.M.A., Krabbendam, L., Martinez-Gonzalez, I., de Bruijn, M.J.W., Golebski, K., Hendriks, R.W., Stadhouders, R., Spits, H., and Bal, S.M. (2019). KLRG1 and NKp46 discriminate subpopulations of human CD117^{+}CRTH2^{-} ILCs biased toward ILC2 or ILC3. J. Exp. Med. *216*, 1762–1776.

Nouri-Aria, K.T., Wachholz, P.A., Francis, J.N., Jacobson, M.R., Walker, S.M., Wilcock, L.K., Staple, S.Q., Aalberse, R.C., Till, S.J., and Durham, S.R. (2004). Grass pollen immunotherapy induces mucosal and peripheral IL-10 responses and blocking IgG activity. J. Immunol. *172*, 3252–3259.

Ott, H., Sieber, J., Brehler, R., Fölster-Holst, R., Kapp, A., Klimek, L., Pfaar, O., and Merk, H. (2009). Efficacy of grass pollen sublingual immunotherapy for three consecutive seasons and after cessation of treatment: the ECRIT study. Allergy *64*, 1394–1401.

Radulovic, S., Jacobson, M.R., Durham, S.R., and Nouri-Aria, K.T. (2008). Grass pollen immunotherapy induces Foxp3-expressing CD4+ CD25+ cells in the nasal mucosa. J. Allergy Clin. Immunol. *121*, 1467–1472.

Renand, A., Shamji, M.H., Harris, K.M., Qin, T., Wambre, E., Scadding, G.W., Wurtzen, P.A., Till, S.J., Togias, A., Nepom, G.T., et al. (2018). Synchronous immune alterations mirror clinical response during allergen immunotherapy. J. Allergy Clin. Immunol. *141*, 1750–1760.e1.

Rolland, J.M., Gardner, L.M., and O'Hehir, R.E. (2010). Functional regulatory T cells and allergen immunotherapy. Curr. Opin. Allergy Clin. Immunol. *10*, 559–566.

Rosser, E.C., and Mauri, C. (2015). Regulatory B cells: origin, phenotype, and function. Immunity *42*, 607–612.

Scadding, G.W., Calderon, M.A., Shamji, M.H., Eifan, A.O., Penagos, M., Dumitru, F., Sever, M.L., Bahnson, H.T., Lawson, K., Harris, K.M., et al.; Immune Tolerance Network GRASS Study Team (2017). Effect of 2 Years of Treatment With Sublingual Grass Pollen Immunotherapy on Nasal Response to Allergen Challenge at 3 Years Among Patients With Moderate to Severe Seasonal Allergic Rhinitis: The GRASS Randomized Clinical Trial. JAMA *317*, 615–625.

Scadding, G.W., Eifan, A.O., Lao-Araya, M., Penagos, M., Poon, S.Y., Steveling, E., Yan, R., Switzer, A., Phippard, D., Togias, A., et al. (2015). Effect of grass pollen immunotherapy on clinical and local immune response to nasal allergen challenge. Allergy *70*, 689–696.

Scadding, G.W., Shamji, M.H., Jacobson, M.R., Lee, D.I., Wilson, D., Lima, M.T., Pitkin, L., Pilette, C., Nouri-Aria, K., and Durham, S.R. (2010). Sublingual grass pollen immunotherapy is associated with increases in sublingual Foxp3-expressing cells and elevated allergen-specific immunoglobulin G4, immunoglobulin A and serum inhibitory activity for immunoglobulin E-facilitated allergen binding to B cells. Clin. Exp. Allergy *40*, 598–606.

Schleimer, R.P., and Berdnikovs, S. (2017). Etiology of epithelial barrier dysfunction in patients with type 2 inflammatory diseases. J. Allergy Clin. Immunol. *139*, 1752–1761.

Seehus, C.R., Kadavallore, A., Torre, B., Yeckes, A.R., Wang, Y., Tang, J., and Kaye, J. (2017). Alternative activation generates IL-10 producing type 2 innate lymphoid cells. Nat. Commun. *8*, 1900.

Shamji, M.H., and Durham, S.R. (2017). Mechanisms of allergen immunotherapy for inhaled allergens and predictive biomarkers. J. Allergy Clin. Immunol. *140*, 1485–1498.

Shamji, M.H., Layhadi, J.A., Achkova, D., Kouser, L., Perera-Webb, A., Couto-Francisco, N.C., Parkin, R.V., Matsuoka, T., Scadding, G., Ashton-Rickardt, P.G., and Durham, S.R. (2019). Role of IL-35 in sublingual allergen immunotherapy. J. Allergy Clin. Immunol. *143*, 1131–1142.e4.

Sharif, H., Singh, I., Kouser, L., Mosges, R., Bonny, M.A., Karamani, A., Parkin, R.V., Bovy, N., Kishore, U., Robb, A., et al. (2019). Immunologic mechanisms of a short-course of Lolium perenne peptide immunotherapy: A randomized, double-blind, placebo-controlled trial. J. Allergy Clin. Immunol. *144*, 738–749.

Stadhouders, R., Li, B.W.S., de Bruijn, M.J.W., Gomez, A., Rao, T.N., Fehling, H.J., van IJcken, W.F.J., Lim, A.I., Di Santo, J.P., Graf, T., and Hendriks, R.W. (2018). Epigenome analysis links gene regulatory elements in group 2 innate lymphocytes to asthma susceptibility. J. Allergy Clin. Immunol. *142*, 1793–1807.

Steveling, E.H., Lao-Araya, M., Koulias, C., Scadding, G., Eifan, A., James, L.K., Dumitru, A., Penagos, M., Calderón, M., Andersen, P.S., et al. (2015). Protocol for a randomised, double-blind, placebo-controlled study of grass allergen immunotherapy tablet for seasonal allergic rhinitis: time course of nasal, cutaneous and immunological outcomes. Clin. Transl. Allergy *5*, 43.

Sugita, K., Steer, C.A., Martinez-Gonzalez, I., Altunbulakli, C., Morita, H., Castro-Giner, F., Kubo, T., Wawrzyniak, P., Rückert, B., Sudo, K., et al. (2018). Type 2 innate lymphoid cells disrupt bronchial epithelial barrier integrity by targeting tight junctions through IL-13 in asthmatic patients. J. Allergy Clin. Immunol. *141*, 300–310.

Sun, C.M., Hall, J.A., Blank, R.B., Bouladoux, N., Oukka, M., Mora, J.R., and Belkaid, Y. (2007). Small intestine lamina propria dendritic cells promote de novo generation of Foxp3 T reg cells via retinoic acid. J. Exp. Med. *204*, 1775–1785.

Taylor, A., Akdis, M., Joss, A., Akkoç, T., Wenig, R., Colonna, M., Daigle, I., Flory, E., Blaser, K., and Akdis, C.A. (2007). IL-10 inhibits CD28 and ICOS costimulations of T cells via src homology 2 domain-containing protein tyrosine phosphatase 1. J. Allergy Clin. Immunol. *120*, 76–83.

Tyurin, Y.A., Lissovskaya, S.A., Fassahov, R.S., Mustafin, I.G., Shamsutdinov, A.F., Shilova, M.A., and Rizvanov, A.A. (2017). Cytokine Profile of Patients with Allergic Rhinitis Caused by Pollen, Mite, and Microbial Allergen Sensitization. J. Immunol. Res. *2017*, 3054217.

van de Veen, W., Stanic, B., Wirz, O.F., Jansen, K., Globinska, A., and Akdis, M. (2016). Role of regulatory B cells in immune tolerance to allergens and beyond. J. Allergy Clin. Immunol. *138*, 654–665.

van de Veen, W., Stanic, B., Yaman, G., Wawrzyniak, M., Söllner, S., Akdis, D.G., Rückert, B., Akdis, C.A., and Akdis, M. (2013). IgG4 production is confined to human IL-10-producing regulatory B cells that suppress antigen-specific immune responses. J. Allergy Clin. Immunol. *131*, 1204–1212.

Vroling, A.B., Jonker, M.J., Luiten, S., Breit, T.M., Fokkens, W.J., and van Drunen, C.M. (2008). Primary nasal epithelium exposed to house dust mite

extract shows activated expression in allergic individuals. Am. J. Respir. Cell Mol. Biol. *38*, 293–299.

Wachholz, P.A., Soni, N.K., Till, S.J., and Durham, S.R. (2003). Inhibition of allergen-IgE binding to B cells by IgG antibodies after grass pollen immunotherapy. J. Allergy Clin. Immunol. *112*, 915–922.

Walker, S.M., Varney, V.A., Gaga, M., Jacobson, M.R., and Durham, S.R. (1995). Grass pollen immunotherapy: efficacy and safety during a 4-year follow-up study. Allergy *50*, 405–413.

Wang, S., Xia, P., Chen, Y., Qu, Y., Xiong, Z., Ye, B., Du, Y., Tian, Y., Yin, Z., Xu, Z., and Fan, Z. (2017). Regulatory Innate Lymphoid Cells Control Innate Intestinal Inflammation. Cell *171*, 201–216.

Yu, H., Huang, X., Ma, Y., Gao, M., Wang, O., Gao, T., Shen, Y., and Liu, X. (2013). Interleukin-8 regulates endothelial permeability by down-regulation of tight junction but not dependent on integrins induced focal adhesions. Int. J. Biol. Sci. *9*, 966–979.

STAR★METHODS

KEY RESOURCES TABLE

REAGENT OR RESOURCE	SOURCE	IDENTIFIER
Antibodies		
anti-human CD1a FITC (HI149)	BioLegend	Cat#300104; RRID:AB_314018
anti-human CD3 FITC (OKT3)	BioLegend	Cat#317306; RRID:AB_571907
anti-human CD14 FITC (HCD14)	BioLegend	Cat#325604; RRID:AB_830677
anti-human CD16 FITC (3G8)	BioLegend	Cat#555406; RRID:AB_395806
anti-human CD19 FITC (HIB19)	BioLegend	Cat#302206; RRID:AB_314236
anti-human CD34 FITC (581)	BioLegend	Cat#343504; RRID:AB_1731852
anti-human CD94 FITC (DX22)	BioLegend	Cat#305504; RRID:AB_314534
anti-human CD123 FITC (6H6)	BioLegend	Cat#306014; RRID:AB_2124259
anti-human FcER1α FITC (AER37)	BioLegend	Cat#334608; RRID:AB_1227653
anti-human TCRαβ FITC (IP26)	BioLegend	Cat#306706; RRID:AB_314644
anti-human TCRγδ FITC (B1)	BioLegend	Cat#331208; RRID:AB_1575108
anti-human BDCA2 FITC (201A)	BioLegend	Cat#354208; RRID:AB_2561364
anti-human IL-17F FITC (Poly5166)	BioLegend	Cat#516604; RRID:AB_10720816
anti-human CD161 PE (HP-3G10)	BioLegend	Cat#339904; RRID:AB_1501083
anti-human NKp44 PE (P448)	BioLegend	Cat#325108; RRID:AB_756100
anti-human IL-9 PE (MH9A4)	BioLegend	Cat#507605; RRID:AB_315487
anti-human HLA-DR PE (L243)	BioLegend	Cat#307605; RRID:AB_314683
anti-human IL-5 PE (JES1-39D107)	BioLegend	Cat#500904; RRID:AB_315139
anti-human CD45 AF700 (HI30)	BioLegend	Cat#304024; RRID:AB_493761
anti-human CD3 AF700 (UCHT1)	BioLegend	Cat#300424; RRID:AB_493741
anti-human IL-17A AF700 (BL168)	BioLegend	Cat#512318; RRID:AB_2124868
anti-human CD161 BV421 (HP-3G10)	BioLegend	Cat#339914; RRID:AB_2561421
anti-human IL-5 BV421 (JES1-39D10)	BioLegend	Cat#504311; RRID:AB_2563161
anti-human STAT3 Phospho BV421(13A3-1)	BioLegend	Cat#651009; RRID:AB_2572087
anti-human IFNγ BV510 (4S.B3)	BioLegend	Cat#502544; RRID:AB_2563883
anti-human CD45 PE-CF594 (HI30)	BioLegend	Cat#304052; RRID:AB_2563568
anti-human IL-13 APC (JES10-5A2)	BioLegend	Cat#501903; RRID:AB_315198
anti-human Siglec-8 APC (7C9)	BioLegend	Cat#347105; RRID:AB_2561401
anti-human CD16 PE-Cy7 (38G)	BioLegend	Cat#302015; RRID:AB_314215
anti-human CD161 BV605 (HP-3G10)	BioLegend	Cat #339916; RRID:AB_2563607
anti-human CD3 AF700 (SK7)	BioLegend	Cat#344822; RRID:AB_2563420
anti-human KLRG1 BV510 (2F1/KLRG1)	BioLegend	Cat#138421; RRID:AB_2563800
anti-human CD127 BV711 (A019D5)	BioLegend	Cat#351328; RRID:AB_2562908
anti-human Lineage cocktail (UCHT1, HCD14, 3G8, HIB19, 2H7, HCD56)	BioLegend	Cat#348801; RRID:AB_10612570
anti-human CD117 PE-Cy5 (104D2)	BioLegend	Cat#313210; RRID:AB_893223
anti-human CRTH2 PE-Dazzle 594 (BM16)	BioLegend	Cat#350126; RRID:AB_2572053
anti-human CD45 PerCP-Cy5.5 (2D1)	BioLegend	Cat#368504; RRID:AB_2566352
anti-human IL-10 (JES3-9D7)	BioLegend	Cat#501412; RRID:AB_493318
anti-human IFNγ BV785 (4S.B3)	BioLegend	Cat#502542; RRID:AB_2563882
anti-human IL-5 PE (JES1-39D10)	BioLegend	Cat#500904; RRID:AB_315139
anti-human IL-13 PE-Cy7 (JES10-5A2)	BioLegend	Cat#501914; RRID:AB_2616746
anti-human T-bet PE-Cy7 (4B10)	eBioscience	Cat#12582582; RRID:AB_925761
anti-human GATA3 PE (TWAJ)	eBioscience	Cat#12996642; RRID:AB_1963600

(*Continued on next page*)

Continued

REAGENT OR RESOURCE	SOURCE	IDENTIFIER
anti-human KLRG1 APC (13F12F2)	eBioscience	Cat#17948842; RRID:AB_2573303
anti-human CD127 PE-Cy7 (R34.34)	Beckman Coulter	Cat#A64618; RRID:AB_2833031
anti-human CD117 PE-Cy5 (104D2D1)	Beckman Coulter	Cat#B96754; RRID:AB_893226
anti-human CRTH2 AF647 (BM16)	Beckton Dickinson	Cat#558042; RRID:AB_2112699
anti-human CD45 APC-Cy7 (2D1)	Beckton Dickinson	Cat#368518; RRID:AB_2616705
anti-human CD94 PerCP-Cy5.5 (HP-3D9)	Beckton Dickinson	Cat#305514; RRID:AB_2565522
anti-human RORγT AF647 (Q21-559)	Beckton Dickinson	Cat#563620; RRID:AB_2738324
anti-human Smad2/Smad3 AF647 (O72-670)	Beckton Dickinson	Cat#562696; RRID:AB_2716578
See Table 5 for TotalSeq Antibody sequences		N/A
Biological Samples		
Healthy human peripheral blood	Sanquin Bloodbank Amsterdam	N/A
Human peripheral blood (non-atopic controls, allergic subjects and immunotherapy-treated)	Royal Brompton Hospital, NHS London, UK	N/A
Human nasal tissue	AMC Amsterdam	N/A
Human AB serum	Merck	Cat#H4522
PA	AMC Amsterdam	N/A
SA RN4220	AMC Amsterdam	N/A
Chemicals, Peptides and Recombinant Proteins		
Recombinant human IL-1b	R&D Systems	Cat#201-LB
Recombinant human IL-2	R&D Systems	Cat#202-IL-500
Recombinant human IL-4	R&D Systems	Cat#204-IL-050
Recombinant human IL-7	Peprotech	Cat# 200-07
Recombinant human IL-17A	R&D Systems	Cat#7955-IL-025
Recombinant human IL-23	R&D Systems	Cat#1290-IL-010
Recombinant human IL-33	R&D Systems	Cat#3625-IL-010
Recombinant human TNF-a	R&D Systems	Cat#210-TA-005
Recombinant human TSLP	R&D Systems	Cat#1398-TS-010
Recombinant human TGF-b	Peprotech	Cat#100-21
Phorbol 12-Myristate 13-acetate (PMA)	Sigma-Aldrich	Cat#P8139
Ionomycin	Merck	Cat#407950
BD Golgiplug Protein Transport Inhibitor	BD Biosciences	Cat#555029
Iscove's Modified Dulbeco's Medium	GIBCO	Cat#21980-065
Roswell Park Memorial Institute (RPMI)1640	GIBCO	Cat#52400-041
Anti-PE microbeads	Miltenyi	Cat#130-048-801
EpCAM microbeads	Miltenyi	Cat#130-061-101
AutoMACS Running Buffer – MACS Separation Buffer	Miltenyi	Cat#130-091-221
MACS separation columns LS	Miltenyi	Cat#130-042-401
Pre-Separation Filters (30 μm)	Miltenyi	Cat#130-041-407
Lymphoprep	StemCell Technologies, Inc.	Cat#07861
Liberase TM	Roche	Cat#5401127001
DNase I	Roche	Cat#11284932001
BD Cytofix Fixation Buffer	BD Biosciences	Cat#554655
BD Phosflow Perm Buffer III	BD Biosciences	Cat#558050
BD PharMingen Stain Buffer	BD Biosciences	Cat#554656
Penicillin-Streptomycin	Roche	Cat#11074440001
1,25 D3-dihydroxivitamin D3	Merck	Cat#D1530
Bronchial Epithelial Cell Growth Medium	Lonza	Cat#CC-3170
PneumaCult-ALI Medium	StemCell Technologies, Inc.	Cat#05001
HyClone FetalClone I Serum	ThermoFisher Scientific	Cat#SH30080.03

(*Continued on next page*)

Continued

REAGENT OR RESOURCE	SOURCE	IDENTIFIER
Critical Commercial Assays		
Foxp3/Transcription Factor Staining Buffer Set	ThermoFisher Scientific	Cat#00-5523-00
Cytofix Cytoperm Fixation Permeablization Kit	Beckton Dickinson	Cat#554714
Duoset ELISA Human IL-10	R&D Systems	Cat#DY217B
Ready-Set-Go IL-5 ELISA kit	ThermoFisher Scientific	Cat#88-7056-77
Ready-Set-Go IL-13 ELISA kit	ThermoFisher Scientific	Cat#88-7439-88
Ready-Set-Go IL-17A ELISA kit	ThermoFisher Scientific	Cat#88-7176-76
Ready-Set-Go IL-8 ELISA kit	ThermoFisher Scientific	Cat#88-8086-88
IL-6 ELISA kit	Invitrogen	Cat#AHC0562
IL-6 Antibody, Biotin	Invitrogen	Cat#AHC0469
Ready-Set-Go GM-CSF ELISA kit	ThermoFisher Scientific	Cat#88-8337-77
NucleoSpin RNA XS kit	Macherey-Nagel	Cat#740902.250
High-Capacity cDNA Reverse Transcription Kit	ThermoFisher Scientific	Cat#4368813
Deposited Data		
Single cell data for ILCs of Grass pollen allergics and non-atopic control		GEO: GSE163367
Single cell data for ILCs of patients receiving either placebo or sublingual grass pollen allergen immunotherapy treatment		GEO: GSE162933
Experimental Models: Cell Lines		
Mouse: OP9 stromal cell line		N/A
Mouse: OP9-DL1 stromal cell line		N/A
Human: H292		N/A
Oligonucleotides		
See Table 4 for qPCR primer sequences		
Software and Algorithms		
GraphPad Prism 7.0	GraphPad	https://www.graphpad.com/
Cytobank (viSNE and FlowSOM)	Cytobank	https://www.cytobank.org/
FlowJo V10	FlowJo	https://www.flowjo.com/
RStudio	RStudio	https://rstudio.com/
BioRad CFX Manager	BioRad	https://www.bio-rad.com/
Partek Flow	Partek	https://www.partek.com/
Other		
Yssel's Medium	In house	N/A

RESOURCE AVAILABILITY

Lead contact

Further information and requests for resources and reagents should be directed to and will be fulfilled by the Lead Contact, Mohamed H Shamji (m.shamji99@imperial.ac.uk).

Materials availability

This study did not generate new unique reagents.

Data and code availability

The accession number for the sequencing data reported in this paper is GEO: GSE163367 and GEO: GSE162933.

EXPERIMENTAL MODEL AND SUBJECT DETAILS

Study participants

The study complied with Good Clinical Practice and was approved by the South West London REC3 Research Ethics Committee and the Research Office of the Royal Brompton and Harefield NHS Foundation Trust. Written informed consent was obtained from every

participant. For *ex vivo* ILC analyses (Figure 5A), untreated grass pollen allergic subjects with seasonal rhinoconjunctivitis (GPA; n = 15) and non-atopic control subjects (NAC; n = 15) were recruited (Table S1). For *in vitro* cross-sectional study (Figures 6A–6J), patients receiving grass pollen SCIT (n = 15; *Phleum Pratense*, Alutard SQ, ALK Denmark), untreated GPA (n = 18), untreated house dust mite (HDM)-allergic subjects (HDMA; n = 6) and NAC (n = 15) were recruited and completed symptom questionnaires. SCIT-treated patients have been receiving immunotherapy for 12 months to 3 years. Inclusion criteria for GPA included those patients who have a medical history of moderate to severe seasonal grass pollen allergic rhinitis for at least two years. This needs to be accompanied by a positive skin prick test ($\geq$3 mm wheal diameter) to grass pollen mixture (ALK-Abello, Hørsholm, Denmark) and elevated specific IgE ($\geq$0.70 kUA/L) level to timothy grass extract without any history of treatment with allergen immunotherapy. NAC enrolled in the study had no prior history of allergic diseases, a negative skin prick test (< 3 mm wheal diameter) to timothy grass and other common aeroallergens and negative specific IgE (< 0.35 kUA/L) level. Participants with a previous history of allergen immunotherapy, chronic or recurrent sinusitis, perennial rhinitis or asthma, current smoker or having a history of smoking > 5 packs per year, a clinical history of other allergies (including symptoms during the tree pollen season), or other significant medical illnesses were excluded from the study. In addition to this, patients enrolled in the study had not used nasal corticosteroids, antihistamines or other anti-allergy medication of at least two weeks prior to assessment. Blood samples from all participants were anonymized and blinded before the laboratory processing. All research laboratory staff were blinded, and all experiments were performed blind.

Tissue samples

Uninflamed nasal inferior turbinates were obtained from patients who underwent corrective surgery for hypertrophy with or without septoplasty. Nasal polyps were obtained from CRSwNP patients undergoing endoscopic sinus surgery. Buffy coats were provided by the blood bank at Sanquin, Amsterdam, the Netherlands. All tissues were collected after subjects provided informed consent in accordance with approved protocols by the Medical Ethical Committee of the Amsterdam UMC, location Academic Medical Center in Amsterdam, the Netherlands.

Study design

In addition to the study participants described above, we used peripheral blood mononuclear cells (PBMCs) from a subset of patients that enrolled in a randomized, double-blind, single-center, placebo-controlled, two arm time course study (Clinical Trial No: NCT02005627; Table S3). The study compared sublingual allergen immunotherapy tablets (GRAZAX®, ALK-Abello Horsholm, Denmark) plus standard treatment (GP-SLIT), with placebo plus standard treatment (PL-SLIT) for a period of 12 months. After 12 months of treatment, total nasal symptom scores were assessed over 60 minutes following grass pollen nasal allergen challenge. Those allergic participants receiving active treatment continued their therapy for another 12 months. Whole blood samples were collected from each subject at various time points throughout the study at baseline, at 1, 2, 3, 4 (coinciding with the peak pollen season), 6, 12 and 24 months of treatment (Steveling et al., 2015). For the purpose of this study, we investigated PBMCs collected only at baseline (PL-SLIT and GP-SLIT), after 6 months (PL-SLIT and GP-SLIT), 12 months of treatment (PL-SLIT and GP-SLIT), and 24 months of treatment (GP-SLIT).

For some experiments (Figures 6K and 6L), we used PB-KLRG1$^+$ ILCs obtained from healthy controls, GP or HDM allergic individuals at baseline and/or after GP or HDM challenge.

METHOD DETAILS

Cells isolation

For isolation of PBMCs, heparinised blood diluted 1:1 with RPMI-1640 media (Invitrogen, UK) was layered on 30% Ficoll-Paque Plus (GE Healthcare, UK) density gradient and centrifuged for 25 minutes at 2200 rpm at room temperature. The peripheral blood mononuclear cell (PBMC) layer was collected, washed and re-suspended in RPMI-1640. The cell viability was greater than 97%, as determined using trypan blue exclusion.

For isolation of cell suspensions from nasal tissues, nasal tissues were manually cut into fine pieces and digested for 45 min at 37 °C with Liberase TM (125 μg/mL) and DNase I (50 U/mL). Cell suspensions were filtered through 70 μm nylon strainer and pelleted by centrifugation (5 min, 400 × *g*).

For isolation of epithelial cells, epithelial cells were obtained by incubating single cell suspension with anti-EpCAM MicroBeads (Miltenyi Biotec) and a positive selection on a magnetic column.

In vitro generation of IL-10-producing ILCs

In some experiments (Figures 1A–1D, 2A–2D, 3B–3F, 4C–4H, 6K–6N, and S7A–S7E), we sorted ILCs from PBMCs. We first depleted PBMCs from CD3, CD14, and CD16 cells and then stained with anti-FITC microbeads (Miltenyi) according to the manufacturer's instructions. Sorting from nasal tissues was performed without pre-enrichment. Cells were stained and sorted using the following monoclonal (all anti-human) antibodies (clone, catalog number): Lin$^-$: (FITC-conjugated CD1a (HI149, 300104), CD3 (OKT3, 317306), CD14 (HCD14, 325604), CD16 (3G8, 555406), CD19 (HIB19, 302206), CD34 (581, 2317520), CD94 (DX22, 305504), CD123 (H6H, 306014), BDCA2 (201A, 354208), FcεRI (AER37, 2273040), TCRαβ (IP26, 306706), TCRγδ (B1, 331208)); AF700-conjugated: CD45$^+$ (HI30, 304024), CD3 (SK7, 501412); PE-Cy7-conjugated: CD127$^+$ (R.3434, A64618); PE-conjugated: CD161$^+$

(HP3G10, 339904); PerCP Cy5.5-conjugated: CD45 (2D1, 368504); BV510-conjugated KLRG1 (2F1/KLRG1, 334608); BV605-conjugated: CD161 (HP-3G10, 339916); BV711-conjugated: CD127 (A019D5, 351328); PE-Cy5-conjugated: CD117 (104D2D1, B96754); PE-CF594-conjugated CRTH2 (BM16, 3450126); and APC-conjugated: KLRG1$^+$ (13F12F2, 17948842) and sorted using a FACSAria (BD) to a purity > 99% either in bulk or as single cells. In some experiments (Figures 4A–4C, 6A, 7A–7J, and S7A–S7G), we enriched pan-ILCs from PBMCs using Pan-ILC isolation kit (StemCell Technologies, Inc.). Purity of enriched ILCs (Lineage$^-$CD127$^+$) were confirmed using flow cytometry (purity > 80%). We define ILCs as: Lin$^-$(CD1a, CD3, CD14, CD16, CD19, CD34, CD94, CD123, BDCA2, FcεRI, TCRαβ, TCRγδ), CD45$^+$ CD127$^+$ CD161$^+$ cells.

Enriched ILCs were seeded in Yssel culture medium supplemented with 5% human AB serum and 1% Penicillin/Streptomycin at a density of 5,000 cells per well and cells were stimulated with IL-2 (15U/mL; R&D Systems), IL-7 (50 ng/mL; Peprotech), IL-33 (50 ng/mL; R&D Systems) and RA (50 nM; Sigma-Aldrich) for 9 days. Cytokines were replenished every 3 days. At day 9, supernatants were collected for measurement of IL-10 (R&D Systems) and cells were stained with the monoclonal mentioned above.

For some bulk and all cloning experiments, cells were cultured on the murine stromal cell line OP9-DL1 (3000 cells were pre-seeded in 96-well round bottom plates one night before coculture). For bulk cultures (500–1000), ILC2s were stimulated for 5–10 days with IL-2 (20 U/mL), IL-7 (10 ng/mL), and various combinations of IL-33, TSLP, and RA (all at a concentration of 10 ng/mL). For bulk culture, fresh cytokines were added after 5 days. For cloning experiments, cytokines and medium were replenished once per week and cells were analyzed after 16-20 days.

ILC clonal expansion

Single ILCs from peripheral blood were sorted by flow cytometry into 96-well round bottom plates pre-seeded with OP9-DL1 cells and stimulated with IL-2 (20 U/mL), IL-7, IL-33 (20 ng/mL each) and RA (10 nM). After 16-20 days, cell cultures were analyzed for intracellular cytokine production (IL-5, IL-13, and IL-10) after PMA and ionomycin re-stimulation or cytokines were measured in culture medium.

Epithelial cells co-cultures with ILCs

Isolated epithelial cells were expanded in culture flasks in BEGM medium (Lonza) until 100% confluency was reached and transferred onto transwells in a 96-well format. Cells were cultured on transwells until 100% confluency in PneumaCult medium (StemCells) according to manufacturer's instructions. Apical medium was then removed, and epithelial cells were exposed to air for additional 20-35 days until differentiated.

The grass pollen allergen (20 μg/mL) was applied on top of the air-exposed cells, while ILCs were added to the basal compartment with growth medium. In co-culture experiments, a mix of Yssel's medium and Pneumacult medium was used. The ILC to epithelium ratio was 1:3. IL-6, IL-8, and IL-10 blocking antibodies were used at 5 μg/mL.

CD4$^+$ T cell co-cultures with ILCs

Peripheral blood CD4$^+$ T cells were co-cultured with KLRG1$^+$ ILCs stimulated with IL-2 and IL-7 or with expanded KLRG1$^+$ ILC clones that produced IL-10 or IL-5 in the ratio of 1:1 to T cells in the presence of IL-2, and in some experiments with IL-4 (20 ng/mL, for CD4$^+$ polarization toward IL-4 production) in Yssel's medium. CD4$^+$ cells were activated with anti-CD3 and/or anti-CD28 (at 2 μg/mL), coated on a microwell plates or added directly to cell culture in the form of beads. Activation of CD4$^+$ T cells was determined by the intracellular staining of IL-4, IFN-γ, or IL-17 and analyzed by flow cytometry. In some samples, anti-IL-10 blocking mAbs were added (at 5 μg/mL).

Intracellular staining for flow cytometry

For experiments involving intracellular cytokine staining, cells were stimulated with PMA (10 ng/mL; Sigma) and Ionomycin (500 nM; Merck) in the presence of Golgi Plug (BD) for 3h at 37 °C. Afterward cells were fixed, permeabilized, and stained using either the Foxp3/Transcription Factor Staining Buffer Kit (ThermoFisher Scientific) or Cytofix-Cytoperm Fixation and Permeabilization Kit (BD Biosciences). Afterward, cells were stained with antibodies for 30 min at room temperature. Samples were acquired on LSRFortessa or FACSCanto II (BD Biosciences) and analyzed with FlowJo software (TreeStar). The following antihuman antibodies were used: FITC-conjugated: PE-conjugated:, IL-5 (JES1-39D107, 500904), GATA3 (TWAJ, 12996642); AF700-conjugated: IL-17A (BL168, 512318); BV421-conjugated: IL-5 (JES1-39D107, 504311), IL-17A (BL168, 512322); BV510-conjugated: IFN-γ (4SB3, 502544); AF647-conjugated: IL-10 (JES3-9D7, 501412), IL-13 (JES10-5A2, 501903), RORγT (Q21559, 563620); PE-Cy7-conjugated: IL-13 (JES10-5A2, 501903), Tbet (4B10, 1282582); PE-Tx-conjugated: IL-10 (JES3-9D7, 501426); BV785-conjugated: IFNγ (4S.B3, 502542). All antibodies were used at 1:200 dilution and were purchased from Biolegend, eBioscience, or Beckman Dickinson.

For some bulk and all cloning experiments, cells were cultured on the murine stromal cell line OP9-DL1 (3000 cells were pre-seeded in 96-well round bottom plates one night before coculture). For bulk cultures (500–1000), ILC2s were stimulated for 8–10 days with IL-2 (20 U/mL), IL-7 (75 ng/mL), and various combinations of IL-33 (20 ng/mL), and RA (0.5 μM). For bulk culture, fresh cytokines were added after 5 days. For cloning experiments, cytokines and medium were replenished once per week and cells were analyzed after 2–3 weeks. Nasal epithelial cells were grown in 75 mL culture flasks in Bronchial Epithelial Cell Growth Medium (Lonza) until confluency or in PneumaCult-ALI medium (StemCell Technologies, Inc.) in the air-liquid interface (ALI) model. For ALI, epithelial cells were seeded onto permeable membrane of culture inserts. The basal epithelial cell surface was in contact with liquid culture

medium, whereas the apical surface was exposed to air. Upon differentiation, cells were exposed to GPA (200 μg/mL) for 24 hours. For co-culture experiments, ILC2s (3000–5000) were added to the culture medium.

IL-5, IL-13, and IL-10 were measured in supernatants by enzyme-linked immunosorbent assay (ThermoFisher Scientific or R&D Systems). Multiple cytokines were detected in some experiments by U-plex technology (Meso Scale Diagnostics).

Quantitative real-time PCR

Total RNA was extracted with a NucleoSpin RNA XS kit (Macherey-Nagel) according to the manufacturer's instructions. cDNA was synthesized with a High-Capacity cDNA Reverse Transcription kit (ThermoFisher Scientific). PCRs were performed in BioRad iCycler (BioRad) with IQ SYBR Green Supermix (Bio-Rad) or with TaqMan Probes. Bio-Rad CFX Manager 3.1 software was used for quantification of expression. All samples were normalized to the expression of control genes encoding GAPDH and β-actin and results are presented in arbitrary units. The sequences of primers used in this study are collected in the Table S4.

Unbiased clustering analysis

Machine learning-driven unbiased analyses (viSNE and FlowSOM) were performed on flow cytometry dataset using Cytobank. Analysis using viSNE and FlowSOM was performed on the ILC population ($CD3^-CD45^+Lin^-$) and cluster setting was set to markers KLRG1, CRTH2, CD161, CD117 and IL-10. FCS files from six patients within the same group were concatenated to generate a representative dataset (FCSConcat2). Red and blue in the viSNE map represents high and low expression of the corresponding markers, respectively. All FlowSOM analysis was performed on a pre-determined metacluster setting of 14. Star plots generated from FlowSOM allows the identification of two pieces of information: 1) size of the cluster nodes representing population abundance; 2) proportion of pie chart within each cluster node representing the expression of markers. The distance between the nodes is proportional to the dissimilarity of expression patterns of nodes or clusters.

Single cell CITE-Seq

For *ex vivo* experiment (Figures 5B–5D), cryopreserved peripheral blood mononuclear cells (PBMCs) were stained with fluorochrome-tagged antibodies for sorting, in parallel with TotalSeq-A antibodies (Table S5). Cells were stained and sorted using the following monoclonal (all anti-human) antibodies (clone, catalog number): CD1a (HI149, 300104), CD14 (HCD14, 325604), CD16 (3G8, 555406), CD19 (HIB19, 302206), CD34 (581, 2317520), CD94 (DX22, 305504), CD123 (H6H, 306014), BDCA2 (201A, 354208), FcεRI (AER37, 2273040), TCRαβ (IP26, 306706), TCRγδ (B1, 331208)); CD45 (2D1, 368504), CD3 (SK7, 501412); CD127 (R.3434, A64618). Stained PBMCs were Flow cytometry-sorted using BD FACS Aria instrument and immediately processed for single cell CITE-Seq. For *in vitro* experiment (Figures 3A and 7H–7J), Lin^- ILCs were enriched from PBMCs as described above using flow cytometry sorting and cultured with IL-2, IL-7, IL-33 and RA for 7 days at 37°C, 5% CO_2. After 7 days of stimulation, ILCs were stained with TotalSeq-A antibodies (Table S5), counted using trypan blue exclusion and immediately processed for single cell CITE-Seq. Single-cell suspensions were loaded onto a Chromium Single Cell Chip and prepared using the Chromium Single Cell 3′ v3 Reagent Kit (10x Genomics) according to the manufacturer's instructions to allow encapsulation with barcoded Gel Beads at a target capture rate of approximately 10,000 individual cells per sample. The captured mRNA was barcoded during cDNA synthesis. Single cell RNA-seq and cell surface protein libraries were prepared for Illumina sequencing according to the manufacturer's instructions using the Chromium Single Cell 3′ Solution (10x Genomics) and Biolegend TotalSeq-A protocol, respectively. All samples for a given donor were processed simultaneously with the Chromium controller and the resulting libraries were prepared in parallel in a single batch. We pooled libraries (RNA and protein) for two separate samples, each of which was barcoded with Illumina sample index, for sequencing in a single lane of Illumina flow cell. The RNA and protein libraries were sequenced on an Illumina HiSeq 4000 with the following conditions: 28-base for read 1, 98-base for read 2, and 8-base for sample index. A minimum of 25,000 and 5,000 reads per cell was sequenced from RNA and protein libraries, respectively.

QUANTIFICATION AND STATISTICAL ANALYSIS

Single cell CITE-Seq data processing

Raw sequencing data was analyzed following CellRanger setting on Partek Flow (Partek). First, we aligned the sequenced RNA reads associated with each sample index to GRCh38 (GENCODE version 28) using STAR after trimming read 2 to remove 3′ poly(A) tails. Number of genes detected per cell, number of UMIs and percentage of mitochondrial genes were plotted, and outliers were removed (number of genes over 2,500, number of UMIs over 12,000, and percent mitochondrial genes over 0.08) to filter out doublets and dead cells. In parallel, we aligned the sequenced protein reads associated with each sample index to a pre-defined assembly consisting of the 15-bp sequence using Bowtie. The number of reads were counted, and the single cell counts were merged to allow analysis of CITE-Seq data. t-SNE analysis was performed, cells were classified, and contaminants removed to allow differential gene and protein analysis by ANOVA. We also perform downstream analysis that allows hierarchical clustering and heatmap generation and biological interpretation was made by pathway enrichment analysis against KEGG database.

Statistics

Statistical analyses were performed using GraphPad Prism v7 (GraphPad Software). Means are given as ± standard error mean (SEM) or, where indicated, as ± standard deviation (SD). Bars plotted in linear scale represents mean and symbols in bar graphs

represent individual patient samples unless otherwise stated in figure legends. Between-group comparisons were performed by using the Mann-Whitney U test for paired samples, one way ANOVA, or Student's t test. Correlation analysis was determined using the Spearman rank method. Data were considered to be statistically significant at * $p < 0.05$, ** $p < 0.01$, and *** $p < 0.001$. For single cell CITE-Seq and RNA-Seq work, statistical analyses were performed using ANOVA on Partek® Flow® software package (Partek). Filtration criteria to identify genes differentially expressed between groups were performed based on False Discovery Rate (FDR) step up of less than 0.05.